LITHOS 430-431 (2022) 106881

Contents lists available at ScienceDirect

LITHOS

journal homepage: www.elsevier.com/locate/lithos

Generation of magmatism under active continental margins: A thermodynamic study of subduction and translithospheric diapirs

Marcos García-Arias [a,b,*], Nathalia Andrea Pineda-Rodríguez [b], Idael Francisco Blanco-Quintero [c], Matthew Jason Mayne [d]

[a] Departamento de Geología, Universidad de Salamanca, Salamanca, Spain
[b] Departamento de Geociencias, Universidad de Los Andes, Bogotá, Colombia
[c] Departamento de Ciencias de la Tierra y del Medio Ambiente, Universidad de Alicante, Spain
[d] Department of Earth Sciences, Stellenbosch University, Stellenbosch, South Africa

ARTICLE INFO

Keywords:
Cordilleran batholiths
Translithospheric diapirs
Subduction
mélange
Density
Thermodynamic modelling

ABSTRACT

A recent model of continental arc magmatism states that subducted sediments mix physically with the oceanic slab basalts in the subduction channel and produce diapirs that ascend through the mantle wedge, undergo melting and relaminate to the base of the continental crust. From here, melt or magma batches ascend through the crust, producing the Cordilleran batholiths and associated volcanism ranging in composition from 0 to 25 wt % maficity ($FeO_t + MgO$) and 44–79 wt% SiO_2, with a gap around 11.5 wt% maficity and 57–60 wt% SiO_2. This model has been predicted by thermomechanical numerical studies and later supported by phase equilibrium experiments; however, thermodynamic modelling to verify whether the composition of the Cordilleran batholiths is reproduced by this model has not yet been carried out to complement the experimental approach. In this article, the evolution of the mélange along the subduction path and during the ascent of the diapirs is investigated, with focus on the conditions of generation of the diapirs, the composition and proportion of melt at the P-T conditions of relamination of the diapirs, the relationship between the basalt:sediment proportion (the composition) of the diapir to this melt composition and proportion and whether the composition of the melts match the Cordilleran batholiths. The key point to test is the process or processes that produce the compositional variability observed in these granitoids. Our findings indicate that (1) parental melts and/or magmas range in maficity from ~1 to ~11.5 wt%, with the compositional gap of the Cordilleran trend representing the most mafic composition possible of the parent, (2) the diapirs are restricted to having 50–60% of sediment component: diapirs with lower sediment contents may be too dense to detach from the slab and mélanges with higher sediment contents may be too less dense to be subducted to the depth of formation of diapirs, (3) melts at 1100 °C and 1.5 GPa from these diapirs have the bulk granodioritic composition of the batholiths, (4) restite unmixing occurs when magma batches segregate from the relaminated diapirs, (5) the lower the temperature of the region of the diapir from which the batch segregates, the higher the restite content, (6) the temperature, by controlling the restite content, is the ultimate factor controlling the compositional trends of Cordilleran batholiths, and (7) fractional crystallization or cotectic evolution is still needed to account for the full compositional range of these batholiths, from the parental 1–11.5 wt% to the observed 0–25 wt% in maficity.

1. Introduction

The continental crust is geochemically intriguing in that it is ultimately formed by partial melting of the mantle, but its andesitic average composition contrasts strongly with the basaltic composition of melts derived from the ultramafic mantle (Cawood et al., 2013; Rudnick and Gao, 2003; Taylor and McLennan, 1985). The current forms of addition of mantellic material to the continental crust are intraplate magmatism, magmatism during rifting, magmatism related to subduction and accretion of island arcs, of which only the latter two are generally accepted to be andesitic in composition (Jagoutz and Kelement, 2015; Kemp and Hawkesworth, 2003; Taylor and McLennan, 1985). The main consequence of this magmatism is the formation of the so-called Cordilleran granitoids (Castro et al., 2010), large batholiths of mostly granodiorites

* Corresponding author at: Office E-2512, Facultad de Ciencias, Plaza de los Caídos s/n, 37008 Salamanca, Spain.
E-mail address: mgarias@usal.es (M. García-Arias).

https://doi.org/10.1016/j.lithos.2022.106881
Received 4 April 2022; Received in revised form 13 September 2022; Accepted 14 September 2022
Available online 20 September 2022

and tonalites but also granites s.s. and some non-granitoid rocks like quartz diorites to gabbros, with a chemical variability matching these lithologies (Fig. 1), and with an age range of several tens to some hundreds of millions of years, such as the South Patagonian batholith (Hervé et al., 2007) or the Sierra Nevada and Peninsular Range batholiths (Lee et al., 2007). They are characterized by a metaluminous to mildly peraluminous composition, a calc-alkaline affinity, enrichment in LILE but depletion in Nb and Ta, and strong variations in the Sr—Nd isotope systems. These compositions suggest contributions from mantellic and crustal materials (e.g. Castro et al., 2010; Kemp and Hawkesworth, 2003; Winter, 2001). Moreover, there seems to be a decoupling between the major element geochemistry of the plutonic rocks and their trace element and isotopic composition, where plutons with a dominantly granodioritic and tonalitic composition have a wide range in the Sr—Nd system, and where more Nd-radiogenic rocks rocks can be richer in silica than less Nd-radiogenic rocks (e.g. Castro et al., 2021; Hervé et al., 2007; Pankhurst et al., 1999). However, there is generally no direct access to the source regions of this magmatism (except for slab-melted blocks in subduction channels, e.g. Blanco-Quintero et al., 2011) and thus any model aimed to explain its composition relies on indirect data (major and trace element and isotopic geochemistry of the continental crust and the Cordilleran magmatism, experimental petrology and thermomechanical models) (Gerya and Yuen, 2003; Lee et al., 2007; Patiño Douce, 1999; Rudnick and Gao, 2003; Taylor and McLennan, 1985).

The most recent model (Behn et al., 2011; Castro, 2014; Castro et al., 2010; Gerya and Yuen, 2003; Hacker et al., 2011; Vogt et al., 2012, 2013), termed 'mélange diapir model' by Castro et al. (2021), explains the Cordilleran magmatism as a consequence of melts derived from mélanges detached from the subducted plate (Fig. 2). In this model, subducted sediments from the accretionary prism (with/without continental crust incorporated by subduction erosion) mix physically with the basalts of the oceanic slab and probably some peridotitic mantle in the subduction channel, forming a mélange of broadly intermediate composition. This mélange is less dense than the overlying mantle wedge and thus density instabilities trigger the ascension of mélange diapirs through the lithospheric mantle (Castro and Gerya, 2008; Gerya and Yuen, 2003). These translithospheric diapirs undergo partial melting by heating from the mantle and decompression, and relaminate at the base of the crust. Hybridization between the mélange and the surrounding mantle at the outer rim of the diapirs may occur (Castro, 2013; Castro and Gerya, 2008; Codillo et al., 2018). Seismic data interpreted as evidence of the presence of diapirs in the mantle wedge has recently been found (Lin et al., 2021). Melts segregated from the relaminated diapirs ascend through this crust, forming the batholiths and associated volcanism (Castro et al., 2010). These melts would have a granodioritic to tonalitic composition, as experimentally determined by Castro et al. (2010), explaining this dominant composition in Cordilleran batholiths, whilst the compositional variability of the Cordilleran granitoids and associated rocks would be the consequence of extraction of residual melts evolved by fractional crystallization or along a cotectic line of descent (Castro, 2013). Compositions not falling in this line of descent could be the consequence of melts derived from the hybridized parts of the diapirs or of some degree of assimilation of the lower crust or country rocks (Castro, 2013). According to this model, the crustal and mantellic contributions come from the subducting slab, which would be an inexhaustible source of these materials, thus explaining the long duration of the Cordilleran magmatism (for instance, 150 Myr for the South Patagonian batholith, Hervé et al., 2007; 80 Myr for the Peruvian Coastal Batholith, Martínez Ardila et al., 2019). The decoupling between the major element and isotopic compositions could be explained as premelting mixing of the basaltic and crustal components, as assimilation of crustal material by mantle melt would couple the SiO_2 content and a more contaminated isotopic signature (Castro et al., 2021). Finally, the mélange diapir model supports the andesite model of Taylor (1967) and Taylor and McLennan (1985) for the growth of continents in that the initial melt composition is intermediate (andesitic) and separation of the silica-rich melt from the silica-poor residuum produces the compositional variation of the continental crust in a silicic upper crust and a more mafic lower crust (Castro et al., 2010).

The mélange diapir model competes against other models to explain the formation of bulk andesitic continental crust from an ultramafic mantle. From its inception, this model has been tested to understand whether the melts produced and their compositional evolution reproduce the compositions observed in Cordilleran batholiths, particularly their compositional variability and distribution from granites s.s. to gabbros (from now on, referred to as the "Cordilleran trend") (Fig. 1). Experimental petrology studies have been made considering variable basalt:sediment proportions in the mélange and several P-T conditions typical of the mantle wedge, including hybridization with the surrounding mantle, and melt compositions and phase proportions have been investigated (Castro et al., 2010, 2013; Castro and Gerya, 2008), but experimental petrology does not allow a study along a continuous P-T path, only at discrete P-T conditions. Thermomechanical modelling (Gerya et al., 2008; Vogt et al., 2012, 2013) does allow the investigation of protracted processes along continuous P-T paths, but this tool is focused on the mechanical behaviour of the bodies considered and cannot produce melt compositions (unless coupled with thermodynamic modelling). Further, thermomechanical modelling treats the basaltic and sedimentary materials as separate bodies and thus cannot study the behaviour of hybrid melts formed from mixtures of basaltic and sedimentary components (i.e. the sedimentary and basaltic components in the mélange are treated separately). An investigation of the full evolution of the melts and their source rocks, from the onset of subduction to the emplacement and crystallization of the melts in the continental crust under continuously variable P-T-X conditions is therefore needed, and thermodynamic modelling is the best suited technique to study this evolution to complement the experimental and themomechanical studies and contribute to their conclusions.

This article will provide a thermodynamic study that focuses on the petrological evolution of the mélange during subduction and the ascent of the diapirs through the mantle wedge. The specific goals are to determine (1) whether partial melting can occur in the subduction channel, (2) the difference in density between the subducted materials and the mantle wedge that triggers the generation and ascent of the translithospheric diapirs, (3) the composition and amount of melt produced at the P-T conditions of the relamination of the diapirs to the continental crust, (4) the similarities between the composition of these melts and the Cordilleran granitoids and associated rocks, (5) whether restite entrainment has an influence on those compositional similarities and (6) the influence of the composition of the source (the basalt:sediment proportion) on these aspects. The key advances of this investigation are determining the basalt:sediment proportion of the mélange that allows it to detach from the subducting slab, determining whether the strongly correlated felsic fraction of the Cordilleran trend is derived only by cotectic evolution or requires other processes, and whether restite entrainment may play a role in such variability, a process very difficult to evaluate under an experimental approach.

2. Composition of granitoids and associated rocks

Cordilleran granitoids and associated rocks (Q-monzodiorites to gabbros) have a maficity (FeO_t + MgO in wt% on an anhydrous basis) that ranges from 0 to 25 wt% and a SiO_2 content from 43 to 79 wt%, whose frequency decreases with increasing maficity and decreasing SiO_2 content (Figs. 1 and 3, Appendix A). The most abundant lithologies (61.5% of the analyses of a personal database, Appendix A) have maficities in the range 2–7 wt% and SiO_2 contents between 65 and 73 wt % (Fig. 3), corresponding to average granites and granodiorites (Le Maitre, 1976). There is a small range (2.7% of the analyses) of maficities, between 10.5 and 12.5 wt% and SiO_2 between 57 and 60 wt%, roughly corresponding to average diorites/andesites (Le Maitre, 1976), in which the amount of analyses is lower than expected according to the

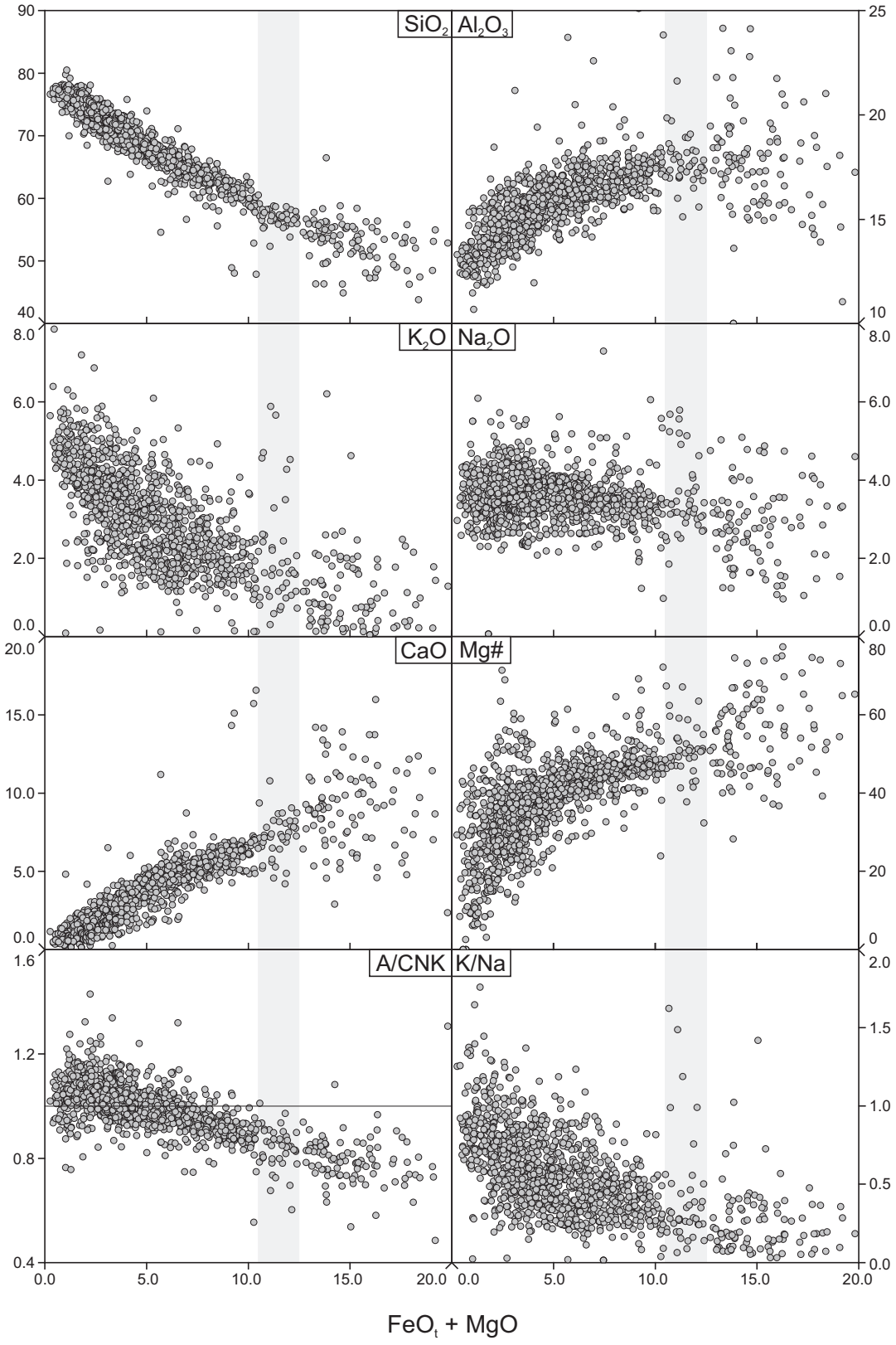

Fig. 1. Compositional trends of Cordilleran granitoids and associated intermediate and mafic rocks with increasing maficity (FeO_t + MgO) for SiO_2, Al_2O_3, K_2O, Na_2O and CaO, and the elemental ratios Mg#, A/CNK and K/Na. The 1044 analyses belong to the personal compilation of M. García-Arias and are shown in Appendix A. The vertical, grey bands correspond to the compositional gap (Fig. 3) that separates the scattered mafic lithologies from the linearly correlated felsic ones (see main text for further information). The horizontal line in the A/CNK panel separates the peraluminous and metaluminous fields.

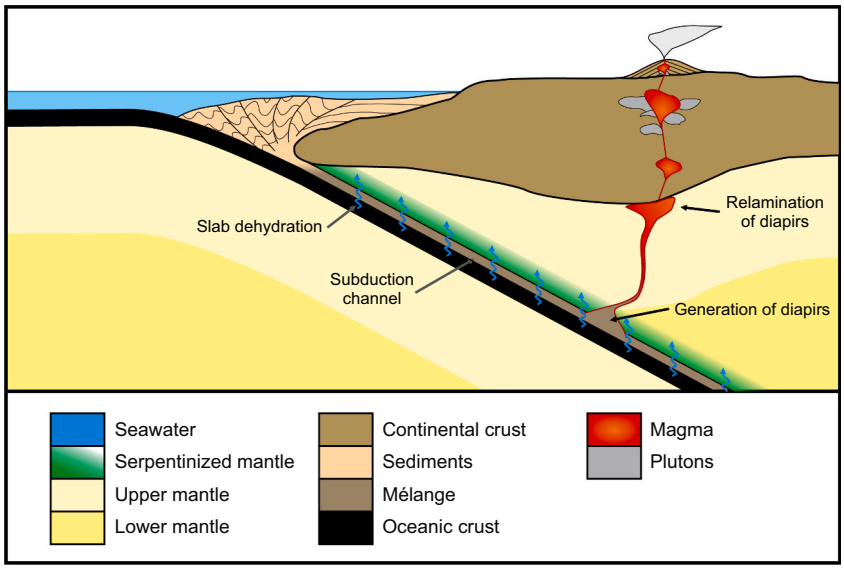

Fig. 2. Simplified sketch depicting the melted mélange model, showing the generation, ascent and relamination of diapirs.

general trend (Fig. 3A, B), a compositional gap found by Castro (2013). In order to assess the statistical significance of this gap in magma compositions, the SiO_2 frequency histogram was trimmed to show only data counts with SiO_2 below 70.5 wt% (no parental magma or melt has a SiO_2 content above this value, see section 5.3) and an exponential regression line was calculated (Fig. 3C). The regression line has an equation of $y = 2.5561e^{0.1385x}$ that fits this reduced dataset with an R2 value of 0.9098. The proposed SiO_2 gap in magma compositions is the largest outlier to this regression line (Fig. 3C), with anomalies of 68%, 27% and 46% (average 47%) of the expected value from the trendline for rocks within the 57–58%, 58–59% and 59–60% SiO_2 ranges, respectively. In other words, the proportion of analyses in the gap is half the expected amount. Moreover, the gap separates the analyses in two groups with different correlations between silica/maficity and other elements and element ratios: a felsic one (90.9% of the analyses) showing a strong linear (straight or curved) correlation, and a more mafic one (6.3% of the analyses) showing a wide scatter (Fig. 1). The large anomalies and the difference in the trend of the analyses indicate that the compositional gap appears to be statistically significant and not a product of sampling bias.

Castro (2013) and Castro et al. (2013) have interpreted this compositional distribution as follows: the composition of the gap represents the composition of the parent melt that, after evolving along a cotectic line of descent, produced fractionated melts (the compositions more felsic than the gap) and melt-depleted residual magmas i.e. cumulates (the compositions more mafic than the gap). These authors derived this interpretation from phase equilibrium relations between experimental melts and mafic residues of systems of bulk andesitic composition at several pressures and bulk H_2O contents. These authors also explain the predominance of felsic rocks over mafic ones as the consequence of fractionation at deep levels, which ensures that the most mafic lithologies are left in the lower crust and that batholiths formed by emplacement of melts at shallower levels are generally more felsic. If this interpretation is right, its application to the mélange diapir model means that this compositional gap could represent the composition of the melts or magmas (andesites/diorites, Le Maitre, 1976) that segregate from the relaminated diapirs, or potentially even the composition of the relaminated diapirs themselves, before further magmatic evolution. The narrow composition of the gap (57–60 wt% SiO_2, 0.7–1.2 wt% TiO_2, 17–19 wt% Al_2O_3, 6.5–8.5 wt% FeO_t, 3.0–5.0 wt% MgO, 6.5–9.0 wt% CaO, 2.5–4.0 wt% Na_2O, 0.6–2.6 wt% K_2O) would then indicate that these initial magmas have a rather restricted composition in their major element geochemistry, implying that some process controlling the basalt:sediment ratio of the diapirs able to segregate from the subducting slab may exist.

There is another intriguing implication of the compositional gap as interpreted by Castro (2013) and Castro et al. (2013). If the mafic group is derived solely by cotectic evolution of magmas with a composition equal to that of the gap and comprises 6.3% of the analyses, and assuming that a parental magma produces an amount of mafic cumulate as low as 10%, then the felsic fractionated part would be 90% of the parental magma, i.e. nine times the amount of the mafic cumulate, representing 56.7% (6.3% times 9) of the felsic analyses of our database. Consequently, 34.2% (90.9% minus 56.7%) of the felsic analyses cannot be explained solely by cotectic evolution and must derive from other processes. We propose, and we will discuss later, that this extra amount represents felsic parental magmas, as the predominance of granites and granodiorites (the composition of melts in the diapirs, Castro et al., 2010) in our database suggests. If the mafic fraction represents >10% of the parental magma, a higher fraction of the felsic fraction cannot be derived solely from cotectic evolution of the gap magmas.

As presented above, the works by Castro (2013) and Castro et al. (2013) appear to produce an apparently contradictory view on the formation of continental arc magmatism to Castro et al. (2010). According to Castro et al. (2010), the melts segregated from the relaminated diapirs have a granodioritic composition and thus they should be the parental melts of the Cordilleran batholiths. In contrast, Castro (2013) and Castro et al. (2013) suggest that the parental magma lies in the compositional gap and thus should have a dioritic composition. Therefore, another advance of our investigation is to evaluate these interpretations, particularly the meaning of the compositional gap.

3. Methodology

3.1. Boundary conditions

Many factors can influence the amount and composition of the melts formed in the diapirs, and even the detachment of diapirs from the subducted mélange: the composition of the basaltic and sediment components, the proportion between these components in the subduction channel, the presence and amount of a mantle component in the mélange, whether this mantle component is incorporated in the subduction channel and/or during the diapir ascent, and the P-T path of the subducting slab, among other factors. Once melts or magmas segregate

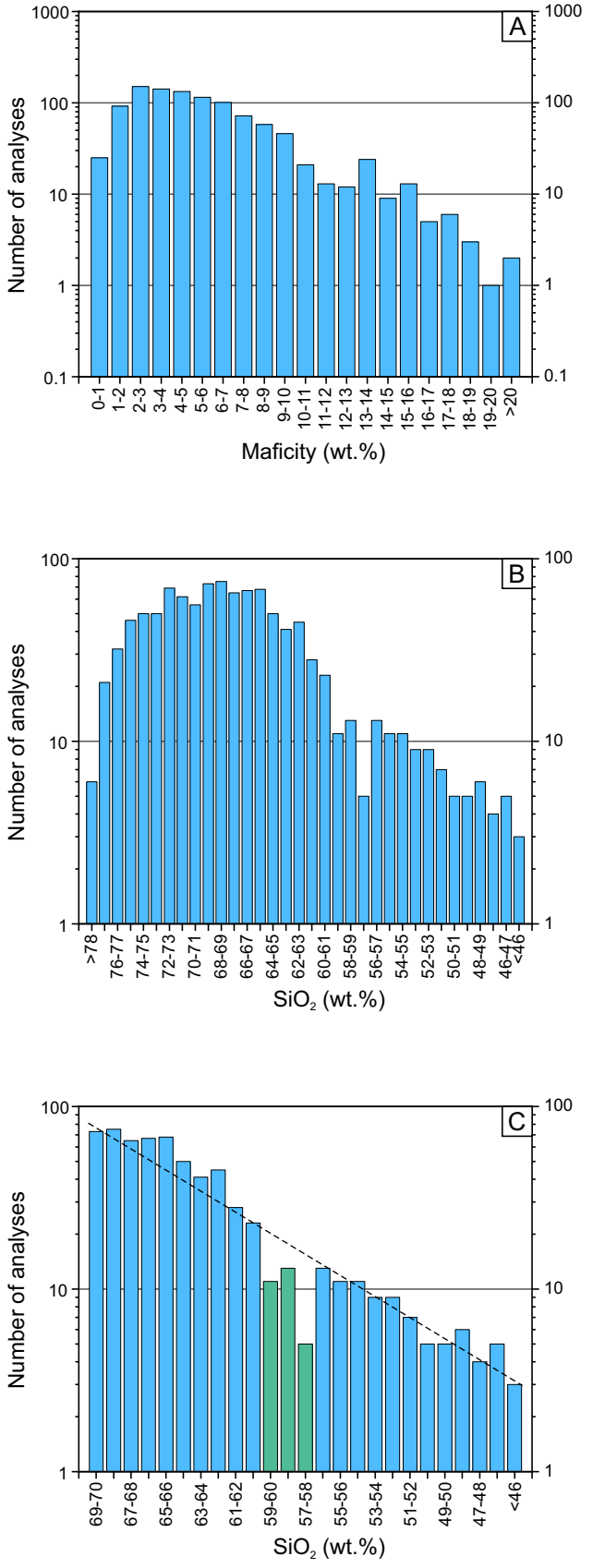

Fig. 3. Frequency of granitoids and associated rocks according to their maficity (panel A) and SiO_2 content (panels B and C) in the database shown in Fig. 1 and Appendix A. Note that the abscises scale in the SiO_2 diagrams has been inverted to showcase the similarity with the distribution of the lithologies in the maficity diagram. The compositional gap in panel C has been highlighted in green; this panel also includes an exponential regression line with equation $y = 2.5561e^{0.1385x}$ and a R2 value of 0.9098. (For interpretation of the references to colour in this figure legend, the reader is referred to the web version of this article.)

(caption on next column)

from the relaminated diapirs, other factors can also contribute to the compositional variability of the Cordilleran batholiths: assimilation of crustal materials by the ascending magmas (either bulk rock, melts or melts + restites), fractional crystallization at crustal levels, and the specific type of fractional crystallization process (filter-pressing, gravitational settling, flow segregation, etc.). Testing every one of these factors at once would produce a very complicated model, difficult to understand due to the many factors involved; consequently, we decided to start with a simplified system as a first-order approximation to which later, in subsequent reports, more layers of complexity (more factors and processes) will be added.

This simplified system will cover the following boundary conditions, which we consider are the primary factors in the composition of the Cordilleran batholiths: only one basaltic composition (a MORB-derived amphibolite), only one sediment composition (an igneous rock with a greywackic composition) and only one P-T path used in thermomechanical models where diapir formation was observed. We chose the basaltic and sediment composition to be the same endmembers of the experimental study of Castro et al. (2010), although we acknowledge the diversity in the sediment composition (chert, pelites, with/without some carbonates). No mantle component was considered, despite being the fundamental source of magmas in the classic model (e.g. Winter, 2001, chapter 17), because Castro and Gerya (2008) experimentally found that the mélange diapir forms a carapace of orthopyroxene ± amphibole that separates the mélange from the mantle and may hinder mélange-hybridization to only the rim of the diapir, making a mantle contribution to the composition of the diapir possibly small. Mixture between the sedimentary and basaltic components in several proportions was considered because we wanted to find the most likely basalt:sediment ratio of the diapirs, if there is any 'preferred' ratio as the restricted composition of the gap implies. The P-T path chosen was one modelled by Vogt et al. (2013) for a 40 Myr old slab subducting at 5 cm/year (Fig. 4). This path was chosen because diapirs rose from the subducting slab in their thermomechanical calculations.

Our investigation covers the evolution of the system until the relamination of diapirs to the base of the crust. Consequently, processes that modify the composition of melts or magmas segregated from the relaminated diapirs were not evaluated.

3.2. *Thermodynamic modelling*

The P-T conditions of the investigated path have been simplified from calculations made by Vogt et al., 2013, their Fig. 6a, first pulse). This path can be divided in four steps: the first one, from 300 °C and 0.63 GPa to 600 °C and 3.3 GPa, corresponds to subduction; the second one, from 600 °C and 3.3 GPa to 1000 °C and 1.7 GPa, corresponds to the ascent and heating of the diapirs through the mantle wedge to the base of a thickened continental crust; the third one, from 1000 °C and 1.7 GPa to 845 °C and 0.64 GPa, corresponds to the ascent of melts through the continental crust, and the fourth and last step, from 845 °C and 0.64 GPa to 765 °C and 0.57 GPa followed by isobaric cooling down to 550 °C, corresponds to the final emplacement and crystallization of the melt. These P-T conditions are similar to those of the calculations of Castro and Gerya (2008) and Gerya and Stöckhert (2006). In this article, only the evolution of the mélange following the first and second steps was investigated.

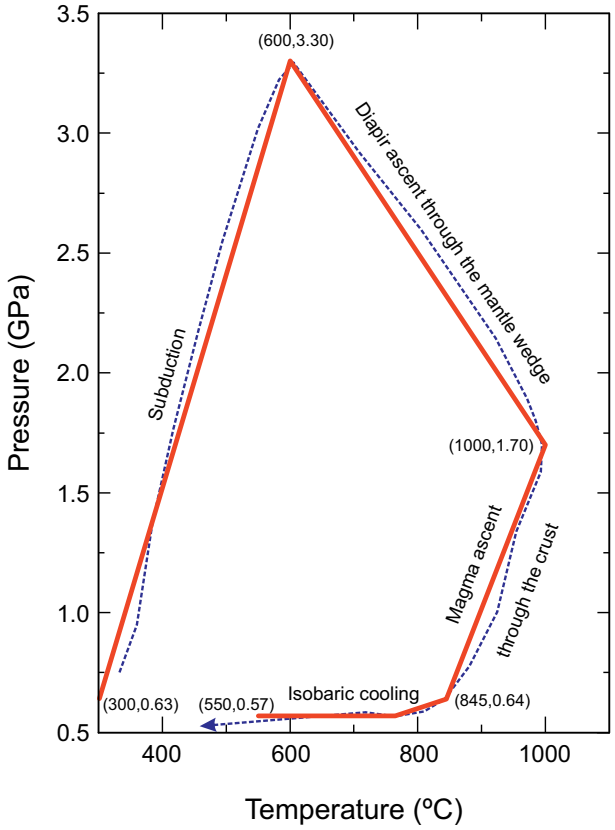

Fig. 4. P-T path of the metamorphic and magmatic evolution of the mélange, from the start of subduction to the emplacement and crystallization of magmas in the continental crust. Blue dashed line: original path from Vogt et al. (2013), their Fig. 6a, blue solid line). Red line: simplified version of the original path, used in the calculations. Coordinates are T (°C), P (GPa). Only the first step (from 300 °C and 0.63 GPa to 600 °C and 3.30 GPa), and second step (from 600 °C and 3.30 GPa to 1000 °C and 1.70 GPa) were used in this investigation. (For interpretation of the references to colour in this figure legend, the reader is referred to the web version of this article.)

The thermodynamic modelling has been carried out using the Perple_X software (Connolly, 2009). The thermodynamic database used is hp633ver.dat, based on the ds6.33 version of Holland and Powell (2011) and subsequent updates. The activity-composition models used are biotite as Bi(HGP), cordierite as Crd(HGP), garnet as Gt(HGP), olivine as O(HGP), orthopyroxene as Opx(HGP) and spinel as Sp(HGP), all from Holland et al. (2018); clinopyroxene as Omph(GHP) from Green et al. (2007); chlorite as Chl(W), chloritoid as Ctd(W), staurolite as St (W) and white mica as Mica(W), all from White et al. (2014) (the model Mica(W) updated to Holland et al., 2018); antigorite as Atg(PN) from Padrón-Navarta et al. (2013); clinoamphibole as cAmph(G) and melt as melt(G), all from Green et al. (2016); epidote as Ep(HP11) from Holland and Powell (2011); feldspars as feldspar from Fuhrman and Lindsley (1988); ilmenite as Ilm(WPH) from White et al. (2000) modified by White et al. (2014); stilpnomelane as Stlp and pumpellyite as Pu, both ideal solutions, from Massonne and Willner (2008); brucite and talc are considered ideal solutions.

The melt model chosen was the "tonalitic" model of Green et al. (2016) instead of the "extended" model of Holland et al. (2018) because García-Arias (2020) found that the latter model contains unacceptably high Ti contents for $P > 2.0$ GPa (preliminary calculations using this model predicted the existence of melt at 600 °C and 3.30 GPa, with a TiO_2 content between 57 and 72 wt% on an anhydrous basis). Moreover, García-Arias (2020) compared the Holland et al. (2018) melt model with that of Green et al. (2016) and found that both produced rather similar results. The clinopyroxene model chosen was the omphacitic pyroxene of Green et al. (2007) instead of the clinopyroxene of Holland et al. (2018) because preliminary calculations with the latter model showed no amphibole for any bulk composition, even basaltic, and amphibole is a common phase in metabasic rocks in subduction environments (e.g. Welch, 2020). The ternary feldspar model of Fuhrman and Lindsley (1988) has been chosen instead of the feldspar models of Holland and Powell (2003) because it is a single feldspar model that does not require an a priori knowledge of the expected compositions of the plagioclase, and because a comparative study between the models (García-Arias, 2020) has demonstrated that the models of Fuhrman and Lindsley (1988) and Holland and Powell (2003) produce very similar results. Other models not belonging to the internally consistent databases and solution model sets of T. Holland and R. Powell have been included to account for phases expected to be stable in this system that do not have models as part of this internally consistent activity model set.

3.3. Bulk compositions

The compositions used in the modelling are a MORB-derived amphibolite as the basaltic endmember (López and Castro, 2001) and the mica-rich Ollo de Sapo orthogneiss chemically resembling a metagreywacke as the sedimentary endmember (Castro et al., 2000). To model the differences in density between the mélange and the overlying mantle, the KLB-1 dry lherzolitic mantle (Takahashi, 1986) has been chosen. The basaltic and sedimentary materials in the subduction channel may be physically mixed, forming separated microdomains with no chemical interaction between them, or may be chemically mixed, forming a single, homogeneous body with a composition between the two endmembers. The main difference between physically and chemically mixed systems is that, for the same basalt:sediment proportion, in the first case the endmembers behave independently of each other and thus the modelling will consider only two compositions, those of the endmembers. In the second case, full chemical homogenization of the components (for instance, due to convection inside the ascending diapirs coupled with heating and partial melting) will produce a single body whose composition will not match neither of the endmembers but will depend on the basalt:sediment proportion. Consequently, five bulk compositions were produced, with a basalt: sediment proportion of 100:0, 75:25, 50:50, 25:75 and 0:100 (in weight proportions). Modal proportions in mechanically mixed systems during subduction with 75:25, 50:50 and 25:75 basalt:sediment proportions were also calculated, but these are a modal balance between the modal proportions of the endmembers and the proportion of each endmember in the physical mix. The mantle composition was investigated as anhydrous and with variable amounts of added H_2O (2 wt%, 3.5 wt%, 7 wt% and 10 wt%) to compare the difference in density between the mélange and the overlying mantle in the subduction stage.

These compositions have been slightly modified in the following ways: MnO has been removed because, at the P-T conditions of the modelling, this element is not relevant for the stability of garnet or other phases. P_2O_5 has also been removed because the thermodynamic database used does not have this component. An amount of CaO proportional to that of P_2O_5 in ideal apatite of formula $Ca_5(PO_4)_3(OH,F,Cl)$ has also been removed, to account only for the CaO present in major phases. FeO_t and H_2O contents have been adjusted as outlined below.

3.3.1. Iron oxidation state

The Fe^{3+}/Fe^{2+} proportion is a crucial parameter in the stability of ferromagnesian phases. Many studies have been devoted to determining the oxygen fugacity of the subcontinental and suboceanic upper mantle due to the fact that Cordilleran magmatism and arc lavas are usually more oxidized (QFM + 0 to +2) than MORB magmatism (QFM-1 to +0.25) (Cottrell and Kelley, 2011; Malaspina et al., 2009; Richards, 2015). The redox state of the subcontinental or subarc mantle wedge is still unknown, as several studies indicate that it has the same oxidation

state as the mantle below ocean ridges (see references below), but whether the source of this oxidized state is due to influx of fluids from the subducting slab (e.g. Brounce et al., 2014; Parkinson and Arculus, 1999) or to partial melting and melt fractionation (e.g. Lee et al., 2010) is still under debate.

If the subducting slab has the same oxidation state as the oceanic crust generated in ocean ridges, we assumed an oxygen buffer of QFM-1 for both the basaltic and sedimentary materials. If the mantle wedge becomes more oxidized due to the input of slab fluids, the mantle before hydration has the same oxygen buffer of the oceanic crust: we assumed an oxygen buffer of QFM-1 for the anhydrous mantle and of QFM + 1 for the variably hydrated mantle. Pressure and temperature are also important variables to calculate the Fe^{3+}/Fe^{2+} proportion of a rock, and thus we chose 550 °C and 2.0 GPa for the mélange (P-T values between the endmembers of the modelled subducting path) and 900 °C and 2.0 GPa for the mantle (average P-T values typical of the suprasubduction mantle wedge). The Fe^{3+}/Fe^{2+} proportion was calculated using the algorithm of Kress and Carmichael (1991) as implemented by Kayla Iacovino (https://www.kaylaiacovino.com/tools-for-petrologists/). This algorithm was created for melts and not for bulk compositions, but García-Arias (2020) showed that the algorithm is a good approximation to estimate the Fe^{3+}/Fe^{2+} proportion of solid rocks.

3.3.2. Water content

Water content is also another important parameter, particularly for the stability of hydrous phases, the position of the solidus and the amount of melt generated, which are some of the objectives of this investigation. In subducting slabs, water is present as both structural water in hydrous phases and free water in the porosity of the rock. We assumed that, at the temperature and pressure of the beginning of the modelling (300 °C and 0.63 GPa), the solid assemblage is fully hydrated (i.e. it contains the maximum possible amount of hydrated phases before the appearance of a free fluid phase) and that most of the porosity has been closed, leaving only minor amounts of free water to guarantee a fully hydrated mineral assemblage. For this reason, T-X_{H2O} calculations at the P-T conditions of the beginning of the modelling have been made for the five starting compositions (100:0 to 0:100 basalt:sediment proportions) to determine the maximum amount of water present in the system to fully saturate it, with only a very small amount of free water (<0.1 wt%). In the case of the mantle composition, 2 wt%, 3.5 wt%, 7 wt % and 10 wt% H_2O were added to the bulk composition and the proportion of the other components was reduced accordingly.

The calculations have been made with a resolution of 1 °C. All free water produced during the subduction due to dehydration has been extracted at every 1 °C; the water produced during the ascent of the diapirs was not removed from the bulk composition: we assumed for simplification that, as both water and the diapir rise together through the mantle wedge, they would not separate and thus water would remain inside the diapir. Consequently, the compositions used in the first step (subduction) and the second step (diapir ascent) differ in that the latter do not contain the water released during subduction and thus have a lower H_2O content. The mélange compositions used in the modelling of the subduction path, including the end-members (original and modified), the anhydrous mantle and the variable hydrated mantle are shown in Table 1 in Appendix B; the mélange compositions used in the ascending diapir path are shown in Table 2 in Appendix B).

4. Results

4.1. Phase assemblage and modal proportions

4.1.1. Subduction stage

The phases present in the modelled systems are shown in Fig. 5 for the physically mixed endmembers and in Fig. 6 for the chemically mixed endmembers (data of the modal proportions in Appendix C). The phases present in part or the whole P-T path are amphibole, chlorite, chloritoid, clinopyroxene, coesite, epidote, garnet, kyanite, lawsonite, paragonite, plagioclase (pure albite), pumpellyite, quartz, stilpnomelane, rutile, talc, titanite and white mica (labelled as Ms. in Figs. 5 and 6). The proportion of quartz, coesite, plagioclase, stilpnomelane and white mica is higher in the calculations with the sediment endmember, whilst amphibole, clinopyroxene, epidote, garnet, paragonite, pumpellyite, rutile and titanite are more abundant in the calculations with the basalt. The basaltic endmember lacks a silica phase between 480 and 550 °C (~2.2–2.8 GPa); white mica is present only at high temperatures/pressures; amphibole only between 325 and 515 °C (0.85 and 2.55 GPa) with the exception of a small gap around 430 °C (1.8 GPa); chloritoid only at around 430 °C (1.8 GPa), and garnet from 430 °C (1.8 GPa) onwards. In the sedimentary endmember, epidote is present only below 326 °C (~0.86 GPa); amphibole only between 400 and 445 °C (1.50–1.93 GPa); chloritoid from 440 to 550 °C (1.89–2.82 GPa), and garnet only above ~500 °C (~2.4 GPa). The phase assemblage of the mélange at 600 °C and 3.3 GPa consists of Cpx + Grt + Lws + Tlc + Coe + Rt + Ms. for the purely basaltic endmember and of Coe + Ms. + Cpx + Grt + Lws + Rt in the purely sedimentary endmember (Appendix C). Eclogitic components (Grt + Cpx) represent ~72% of the basaltic mélange but only ~29% of the sedimentary mélange. It must be remembered that, in the physically mixed mélanges (Fig. 5), the proportion of each phase will range between those in the endmembers but the maximum P-T range of stability of the phases will be a combination of the ranges of those stabilities in the endmembers.

Significant differences exist between the physically and chemically mixed systems for the same basalt:sediment ratio. In the chemically mixed systems, the proportions of stilpnomelane and lawsonite are higher (at the expense of chlorite and talc); amphibole is more abundant and ranges from ~390 °C to ~500 °C (~1.4–2.4 GPa) and from 530 to 570 °C (~2.7–3.0 GPa); paragonite is more abundant; epidote is generally restricted to low temperatures and pressures. Other mineral phases show comparable proportions and P-T ranges of stability compared to the physically mixed systems.

Water is released in the subduction step in two stages, the first one below 325 °C and the second stage above 480 °C for the pure endmembers and above 520 °C for the chemically homogeneous mixtures (Figs. 5 and 6, Appendix C). The amount of water released in the first stage is very small, always below ~0.3 wt%. The amount of water released in the second stage is much higher, at ~2.8 wt% for the basalt endmember, ~1.1 wt% for the sediment endmember and between ~1.5 wt% to ~4.0 wt% for the chemically homogeneous mélanges, with water increasing with increasing basaltic component. The full amount of water released from the pure basalt and sediment mélanges equals to ~55% and ~ 41% of the H_2O content of the respective bulk compositions, whilst for the chemically equilibrated systems this amount ranges from ~43% to ~68%, again increasing with increasing basaltic component.

4.1.2. Diapir ascent stage

The phase assemblages and proportions of the five investigated compositions for the diapirs are shown in Fig. 6 and Appendix C. Alkali feldspar, amphibole, clinopyroxene, coesite, garnet, ilmenite, kyanite, lawsonite, melt, plagioclase, quartz, rutile, talc, water and white mica (this latter labelled Ms. in Fig. 6) are present in some or all five compositions. The feldspar predicted by the calculations with the 0:100 basalt:sediment composition appears sometimes as alkali feldspar plus plagioclase and sometimes as a single ternary feldspar (labelled Fsp in Fig. 6). With increasing sedimentary component in the bulk composition, the proportion of clinopyroxene, garnet, kyanite, lawsonite, rutile and water decreases whilst the proportion of quartz/coesite, both feldspars, ilmenite and white mica increases. Water and white mica are completely consumed in the melting process, with water consumed at the solidus except at a basalt:sediment proportion of 100:0 (vice versa for white mica); clinopyroxene is another main melt-producing mineral phase. The temperature of the solidus is similar for all five compositions,

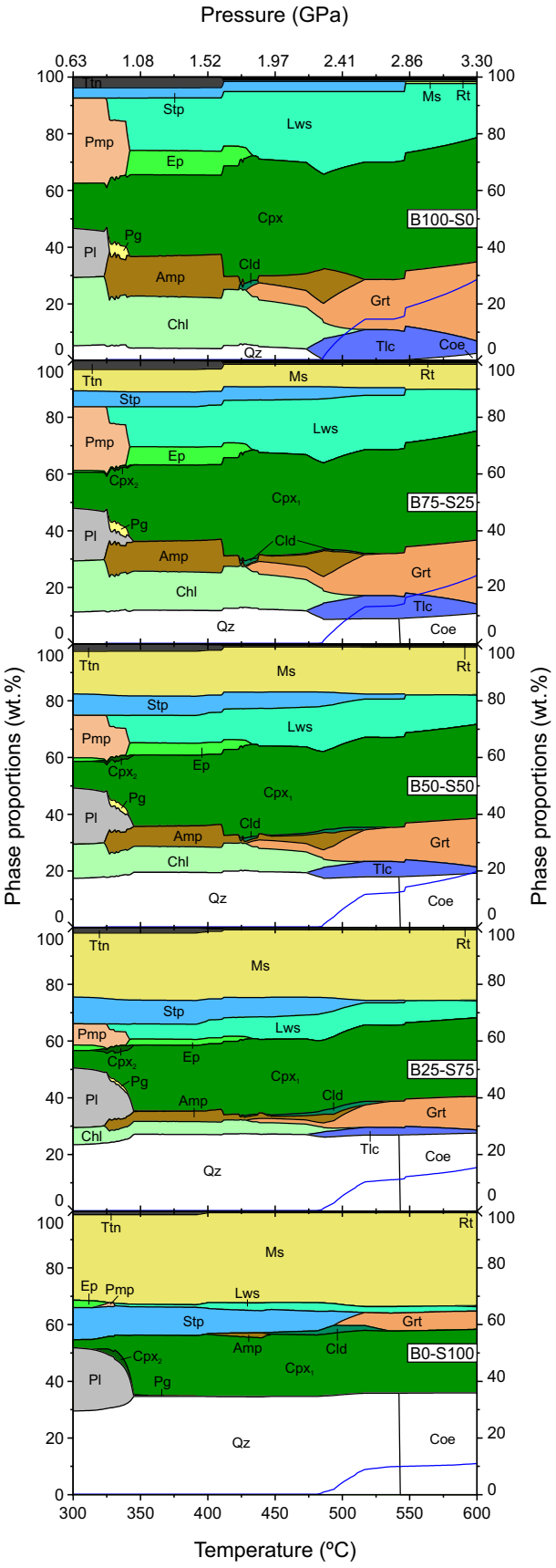

(caption on next column)

Fig. 5. Modal proportions in wt% of the phases predicted by the calculations in the subduction step and the physically mixed mélanges. Blue solid line is the total accumulated water released by each composition, multiplied by 10. BX-SY indicate the relative proportions of basalt (B) and sediment (S) in the mélange. Mineral abbreviations according to Whitney and Evans (2010). When two clinopyroxenes of different composition are present, they were labelled Cpx_1 and Cpx_2. Temperature is shown at the bottom of the figure, pressure at the top. (For interpretation of the references to colour in this figure legend, the reader is referred to the web version of this article.)

decreasing slightly with increasing sedimentary component (from ~835 °C for the 100:0 basalt:sediment ratio to ~820 °C for the 0:100 ratio). The pressure of the solidus increases from 2.36 to 2.43 GPa (equivalent in depth to ~82.5 to ~85.0 km, within the 60–95 km range of seismically detected diapirs, Lin et al., 2021) with increasing sedimentary component. At 1000 °C and 1.7 GPa, the end of the modelled path, the phase assemblage consists of Melt + Grt + Rt + Ilm ± Cpx ± Amp ± Pl/Fsp ± Qz ± Ky. The proportion of melt at these P-T conditions increases with increasing sedimentary component, from ~28 wt% (~38 vol%) at a basalt:sediment 100:0 proportion to ~45 wt% (~51 vol%) at a 25:75 proportion, then decreasing to ~35 wt% (~39 vol%) at a 0:100 proportion (Table 3 in Appendix B).

4.2. Slab and mantle density

To study the variation in density of the modelled mélanges and the overlying mantle, new calculations with the composition of the anhydrous and variably hydrated mantle have been made. The P-T path is the same as that of the modelled mélanges except that, at the same pressure, the mantle was chosen to be 100 °C warmer than the mélange. This increment in temperature was decided because the mantle wedge is warmer than the subducting slab and because the thermomechanical modelling of Vogt et al. (2012, 2013) showed that the layer of mantle wedge just atop the subduction channel is on average 100 °C warmer than the underlying melange. The phase proportions of the mantle are reported in Appendix D; the density of the mélanges and mantle are reported in Appendix E.

The mélange densities reported in Fig. 7A correspond to the solid fraction even when a free fluid phase is present. Given the very low amount of water present at any P-T condition in the calculations, the influence of such small amount of water in the bulk density of the mélanges should be minimal. However, the upper layer of the subduction channel (the closest to the mantle wedge) may contain significant amounts of water due to water infiltration from the lower layers and thus its bulk density will be lower (Fig. 7B), meaning that our calculated 'dry' mélange densities should be considered upper estimates.

Density increases generally smoothly with temperature/pressure for all modelled mélanges, with some sharp increments (Fig. 7A and Appendix E). The first increment, between 325 and 345 °C (0.86–1.03 GPa), is related mainly to the consumption of albite and the formation of amphibole and/or clinopyroxene. The second increment occurs only in the chemicaly homogeneous mélanges at ~390 °C (~1.43 GPa), and is related to the formation of amphibole and lawsonite. The third increment occurs progressively between 475 and 515 °C (2.19–2.54 GPa) and is related to the formation of garnet (plus talc in the basalt endmember). The fourth and last increment occurs at 543–548 °C (2.79–2.83 GPa) and is related to the formation of more garnet and talc in the pure basalt endmember and the transition from quartz to coesite in the pure sediment endmember (Fig. 7). It is expected that physically mixed basalt+sediment mélanges have densities between the endmembers.

Regarding the mantle, density also increases smoothly with temperature and pressure at constant bulk H_2O content and decreases with increasing bulk H_2O content at constant temperature and pressure (Fig. 7). Once the mantle becomes fully hydrated and a free fluid phase is present, the density of the solid fraction becomes constant. Several minor increments appear at 460–480 °C (1.17–1.34 GPa), related to the

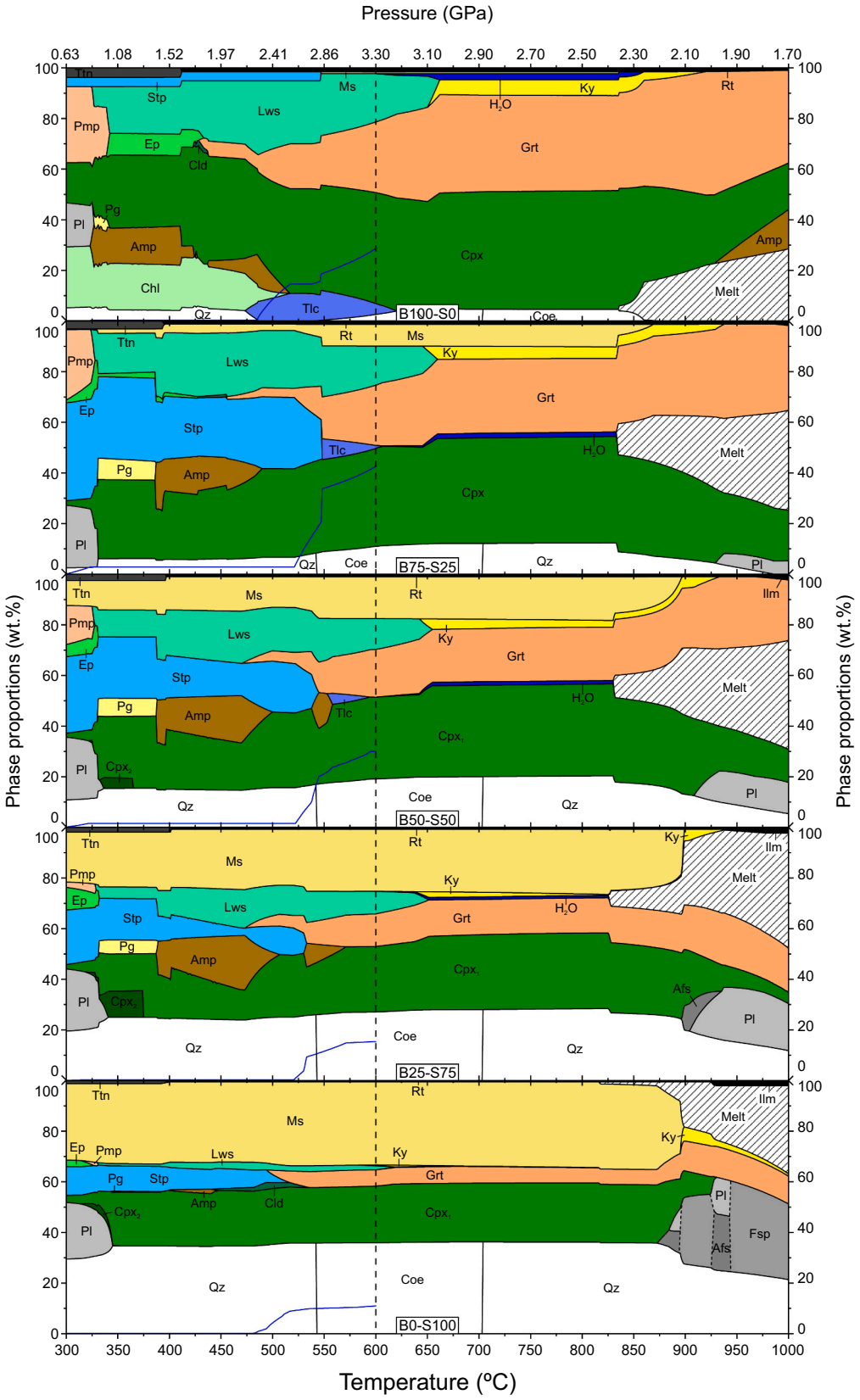

Fig. 6. Modal proportions in wt% of the phases predicted by the calculations in both the subduction and ascending diapir steps in chemically mixed mélanges. BX-SY indicate relative proportions of basalt (B) and sediment (S) in the mélange. Mineral abbreviations according to Whitney and Evans (2010) except for melt. When two clinopyroxenes of different composition are present, they were labelled Cpx_1 and Cpx_2. Temperature is shown at the bottom of the figure, pressure at the top.

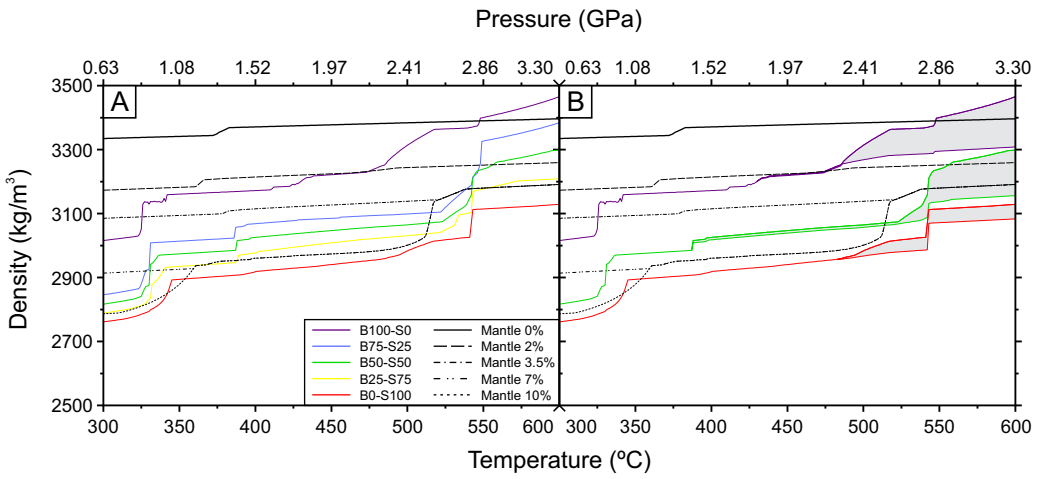

Fig. 7. A) Densities of the solid fraction of the modelled chemically homogeneous mélanges (coloured lines), anhydrous mantle (black solid line) and variably hydrated mantle (other black lines). B) Same as A, but highlighting the difference in density between the mélanges with all free water extracted and the same mélanges if the free water is not extracted. Note that the densities of the mantle were calculated at 100 °C higher than the temperature of the mélanges (see main text for details). Also note that some lines for the hydrated mantle merge when the mantle becomes fully hydrated, as they have the same mineral assemblage with the same proportions and thus the same density.

formation of garnet and/or orthopyroxene ± clinopyroxene, and several substantial increments at 410–460 °C (0.72–1.16 GPa) and 580–635 °C (2.23–2.72 GPa) when the mantle is fully H_2O-saturated due to several events of consumption of antigorite ± amphibole and formation of olivine (Fig. 7 and Appendix D).

The density of the anhydrous mantle is always higher than that of the mélanges except for the pure basalt endmember at $T > 550$ °C ($P > 2.85$ GPa), and a fully hydrated mantle has a similar density to that of the 25:75 basalt:sediment mélange at the highest temperatures/pressures investigated (Fig. 7).

4.3. Melt composition

The melts at 1000 °C and 1.7 GPa are silica-rich (67.8–70.4 wt% on an anhydrous basis), felsic (FeO + MgO = 1.1–1.7 wt%), slightly peraluminous (A/CNK = 1.04–1.06, although the melt from the 0:100 basalt:sediment diapir has a value of 1.30) and with a highly variable K/Na ratio (0.03–1.08) (Fig. 8, Table 3 in Appendix B), falling near the composition of granites s.s. (Le Maitre, 1976). These melts have a restricted composition (particularly in their maficity) despite the wide basalt:sediment ratio of the bulk composition of the diapirs. With the exception of K_2O and Na_2O (and thus the K/Na ratio), the difference in composition between the melts from diapirs with 25:75, 50:50 and 75:25 basalt:sediment proportions is smaller than the difference in composition between any of these melts and the melts from the pure endmembers (Fig. 8). Compared to the Cordilleran granitoids and associated rocks, all melts have a maficity similar to the most felsic rocks but are silica-poorer and alumina- and CaO-richer, plotting away from the Cordilleran trend. Moreover, melts from the diapirs with a basalt:sediment proportion of 100:0 and 75:25 are also K_2O-poorer and Na_2O-richer than granitoids of equivalent maficity. All melts have a maficity lower than the compositional gap of 10.5–12.5 wt% (Fig. 8).

5. Discussion

5.1. Rise of mélange diapirs

No melt phase appeared in the subduction stage but it did appear during the ascent of the diapir through the mantle wedge (Fig. 5, Appendix C). This may be caused by the low temperatures considered in the modelling (below 600 °C) and because melt proportion decreases with increasing pressure (e.g. Castro et al., 2000; Patiño Douce and Beard, 1995; although see Patiño Douce (2005) for a backbending of the solidus of a tonalite system at $P > 2.7$ GPa). These results are in agreement with exhumed fragments of subducting slabs worldwide, where partial melting of the subducting slab has been described in only a few places (e.g. Blanco-Quintero et al., 2011; Rossetti et al., 2010; Sorensen and Barton, 1987). The results also agree with the thermomechanical calculations of Vogt et al., 2013, their Fig. 6a), which predicted the presence of a melt phase only during the ascent of the translithospheric diapir. Therefore, partial melting in the subduction channel is not the mechanism that triggers the formation of the diapirs (at least not under the chosen P-T conditions for the subduction path), and thus this trigger must be the difference in density between the mélange and the overlying mantle.

This difference in density decreases with increasing pressure and temperature, with increasing basaltic component in the mélange and with increasing hydration of the mantle, but increases with increasing free water content in the mélange (Fig. 7). This difference is smallest at the highest P-T conditions of the modelled subduction path, which are the conditions at which the translithospheric diapirs form according to the thermomechanical models of Castro and Gerya (2008), Gerya et al. (2008) and Vogt et al. (2012, 2013). Above 2.82 GPa and 547 °C, the purely basaltic (eclogitic) dry mélange is denser than the mantle (Appendix E) and thus would be unable to produce diapirs. Only if the mélange is highly hydrated will it be less dense than the mantle (Fig. 7B), but it seems highly unlikely that the slab is hydrated whilst the mantle is not. Given the decrease in mantle density with increasing hydration at constant P-T conditions (Fig. 7), we consider that diapirs would not be able to form when the mantle contains >3.5 wt% H_2O unless the mélange is nearly pure sediment, a highly unlikely composition. Consequently, for mélange to be buoyant and diapirs to form, they must contain both basaltic and sedimentary components and the mantle must not be fully hydrated. This conclusion is in agreement with mass balance calculations of the isotopic compositions of the North Patagonian batholith, with sediment contents in the range of 20–40% for the plutons in the Aysén region and 40–70% for the plutons in the Bariloche region, and with a drastic reduction in magma productivity in the same batholith during the Late Cretaceous when the tectonic coupling between plates did not favour sediment/crust erosion, i.e. when the basaltic component in the mélange was higher (Castro et al., 2021).

We speculate that another factor in promoting the formation of diapirs could be that at around 600 °C a threshold in the ductility of the mélange is crossed, such that the shear forces with the overlying mantle are strong enough to squeeze some mélange out and form the embryo of a diapir. This change in the ductility of the mélange with increasing temperature may be a consequence of the infiltration to the upper layer of the subduction channel of fluids derived from the lower layers of the channel; as indicated above, the amount of water released increases drastically after 500–525 °C (Figs. 5 to 7).

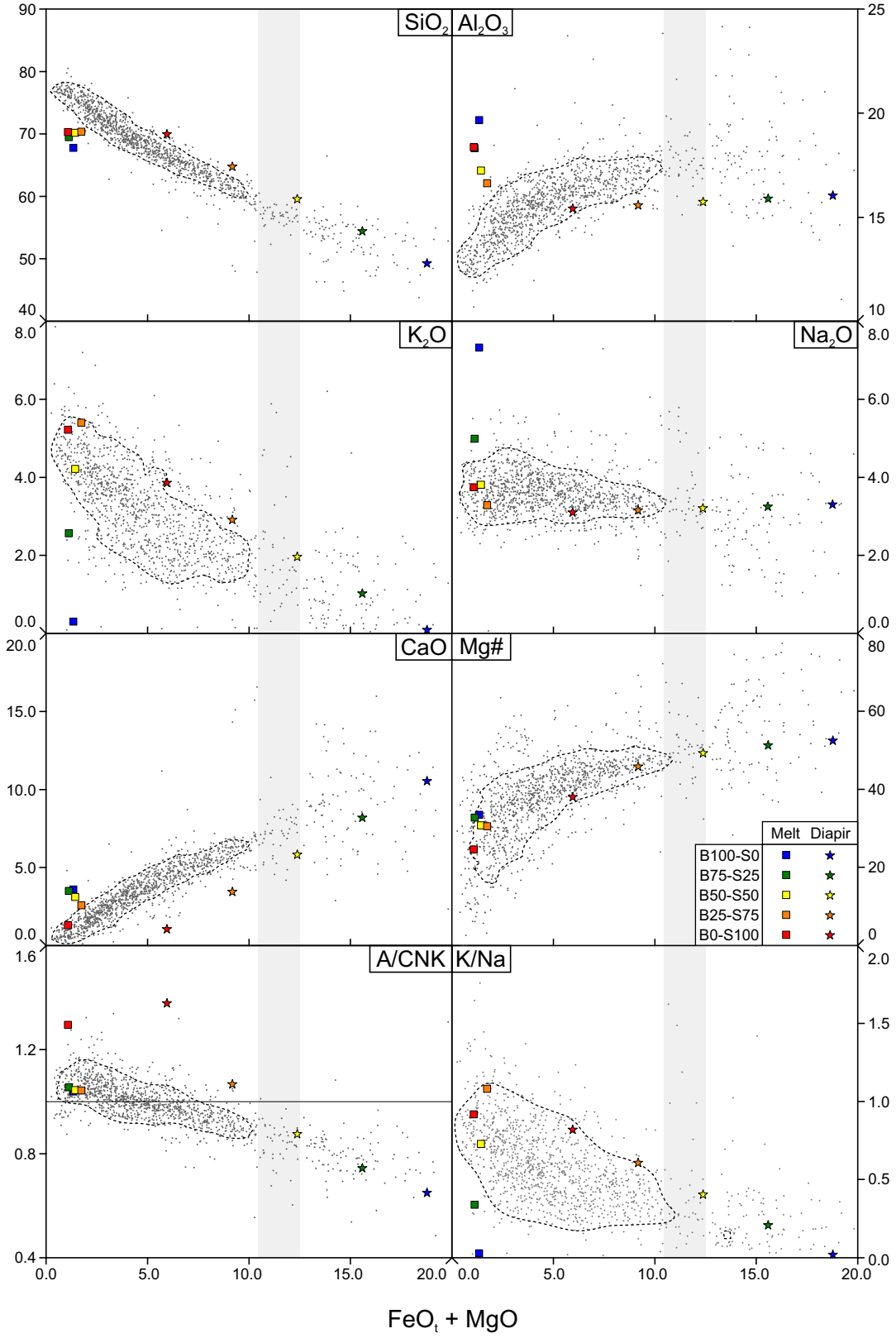

Fig. 8. Composition of the melts modelled at 1000 °C and 1.7 GPa (squares), plotted against the Cordilleran trend. The composition of the sources (stars) is also included. The dashed line contours 80% of the granitoids in a kernel density distribution. Note that not a single modelled melt composition plots within the contour line for all elements and element ratios.

5.2. Melt composition

The similarity in the composition of the melts from diapirs containing both endmembers, and their differences from melts generated from diapirs containing only one endmember, is in agreement with the experimental findings of Castro et al. (2010). In our modelling, the melts from hybrid sources at the P-T conditions of relamination are in equilibrium with a mineral assemblage of Grt + Cpx + Pl plus minor Rt + Ilm ± Qz ± Ky, which is quite similar to the Grt + Cpx + Pl plus minor Hbl + Opx + Rt mineral assemblage of the experimental run of Castro et al. (2010) at 1000 °C, 1.5 GPa and a 50:50 basalt:sediment proportion in the starting composition, with the differences ascribed to the different pressure of the experiment and the modelling. The departure of these melts from the Cordilleran trend agrees also with the experimental findings of Castro et al. (2010) because (1) the experimental melts at 1100 °C and 1.5 GPa of Castro et al. (2010) have a much closer composition to granodiorites and tonalites; (2) the H_2O content of the modelled melts (4.68–7.46 wt%) is well above the maximum content of 2 wt% in parental magmas according to the estimations of Castro (2013) and the maximum contents of 2.0–2.5 wt% in melts at the P-T conditions of magma chambers (e.g. Kovalenko et al., 2000; Okumura, 2011), and (3) fractional crystallization of such magmas cannot produce the whole compositional variability of the Cordilleran magmatism, as the maximum maficity of fractionated cumulates produced by filter-pressing of magmas (the model advocated by Castro, 2013 for Cordilleran plutons) is only twice the maficity of the parental melt or magma (García-Arias and Stevens, 2017a).

If the parental melt or magma needs to be more mafic than the melts modelled at 1000 °C and 1.7 GPa, two scenarios not involving a mantle component in the source (a scenario not considered in this simplified system) may produce this increase in maficity: melting at higher temperatures and/or lower pressures, and restite entrainment.

5.2.1. Modelling at higher temperatures and lower pressures

Modelling at higher temperature and lower pressures means departing from the chosen P-T path. However, the relaminated diapirs cannot have a uniform temperature and pressure due to their volume, as considered by Castro et al. (2010), their Fig. 11). Additionally, different P-T conditions are also supported because the P-T paths vary in subductions zones according to the age of the lithosphere, the maturity of the subduction zones and/or the subduction rates (e.g. Blanco-Quintero et al., 2011). Moreover, Vogt et al. (2013) have made a total of 16 calculations and the P-T conditions of relamination of the diapirs vary along a range, further supporting the reasoning that the diapirs do not have uniform P-T conditions. Therefore, the P-T conditions of the path of Vogt et al. (2013) used in this model can be understood as an average of the conditions of the whole diapir. For these reasons, new calculations at 1000 °C and 1.5 GPa and 1100 °C at 1.5 and 1.7 GPa were made to cover a range in pressure and temperature aimed to increase the maficity of the melts.

The results of the new calculations are shown in Fig. 9 and Table 3 in Appendix B. The new melts are more mafic than the melts at 1000 °C and 1.7 GPa because increasing temperature increases the solubility of Fe and Mg in the melt and possibly because decreasing pressure hinders the formation of garnet, thus allowing more Fe and Mg in melt. The new melts also have a restricted composition for variable basalt:sediment proportions at constant P-T conditions, particularly in their maficity contents, as in the case of the melts at 1000 °C and 1.7 GPa and in agreement with Castro et al. (2010). Only the melts at 1100 °C (both pressures) from the diapirs with a basalt:sediment proportion of 50:50 and 25:75 plot within the Cordilleran trend for all considered elements and element ratios, again in agreement with Castro et al. (2010). These melts are silica-rich (67.0–69.1 wt% on an anhydrous basis), relatively felsic (FeO + MgO = 3.6–4.9 wt%), subaluminous (A/CNK = 0.99–1.01) and relatively sodic (K/Na = 0.45–0.64), and have a composition close to adamellites (monzogranites) and granodiorites (compositions from Le Maitre, 1976). The H_2O content of these melts (2.5–3.1 wt%), although lower than in the 1000 °C/1.7 GPa experiments, is still higher than the maximum amount of 2 wt% estimated by Castro (2013) but closer to the maximum content of 2.5 wt% of andesitic melts in magma chambers (e.g. Kovalenko et al., 2000; Okumura, 2011). However, these melts are too felsic to plot in the compositional gap of 10.5–12.5 wt% maficity and 57–60 wt% SiO_2 (Fig. 9, Table 3 in Appendix B) and thus, according to the model of Castro (2013) and Castro et al. (2013), could not be the parental melts of the Cordilleran granitoids and associated rocks. Consequently, these melts can be responsible for the main granodioritic composition of Cordilleran batholiths, but they cannot produce the whole compositional variability of Cordilleran magmatism by equilibrium or fractional crystallization given the limit in maficity of fractionated bodies controlled by the composition of the parental magma (García-Arias and Stevens, 2017a).

5.2.2. Restite entrainment

Restite entrainment is a process that can increase the Ca, Fe, Mg and Ti contents of a magma without involving variations in temperature or pressure. Segregation of a single melt phase is favored over segregation of a magma because magmas are denser and more viscous than melts, which explains why felsic rocks are more abundant than more mafic ones in S-type granitic batholiths (e.g. García-Arias, 2018; García-Arias and Stevens, 2017). This abundance-maficity distribution is also observed in Cordilleran granitoids and associated rocks (Fig. 3A), so investigating this process is worthwhile. Three processes of restite entrainment have been discussed in the literature: (1) restite unmixing (White and Chappell, 1977), in which all minerals present in the system entrain to the melt in their stoichiometric proportions; (2) peritectic assemblage entrainment (PAE; Stevens et al., 2007), in which only the peritectic mineral assemblage is entrained, and (3) selective restite entrainment (SRE; García-Arias and Stevens, 2017), in which all minerals entrain to the melt but the peritectic fraction dominates over the non-peritectic one. Which specific process takes place depends on the melt:mineral proportion in the partially melted system: if minerals are in suspension within the melt, the whole mineral assemblage is able to be co-segregated (restite unmixing is favored); however, if the reactant minerals are interlocked and only the peritectic fraction is in suspension in the melt, this fraction is more mobile and thus more able to be co-segregated (PAE and SRE are favored). Therefore, the key in choosing a specific restite entrainment process to model lies in the amount of melt present in the system.

The melt amount of the diapirs at the four P-T conditions evaluated ranges from ~38 vol% (~29 wt%) to ~89 vol% (~8 wt%, Table 3 in Appendix B). The lowest melt proportion is close to the ~0.4 melt fraction (40 vol%) of Rosenberg and Handy (2005) at which the interlocked framework breaks down, meaning that the amount of all modelled melts lies always at or above this threshold and thus that all minerals are in suspension in the diapirs. This mineral suspension makes segregation of only the melt phase from the relaminated diapirs very unlikely, implying that mineral entrainment (of the restite unmixing type) may be more common than expected. Calculations made by Castro (2020) on the composition of I-type granitoids modified by the entrainment of several restites support this affirmation. Consequently, the composition of magmas produced by restite unmixing with 0, 20 and 40 wt% entrained minerals at 1000 °C/1.7 GPa and 1100 °C/1.5 GPa (the conditions that produced the least and most mafic melts, respectively) will be evaluated (Figs. 10 to 12 and Table 4 in Appendix B).

Many restite-bearing magmas from diapirs with both basaltic and sedimentary components, and particularly those from diapirs with a basalt:sediment proportion of 50:50, plot within the Cordilleran trend for all considered elements and element ratios, including magmas formed at 1000 °C and 1.7 GPa (Fig. 10), with compositional trends that mimic the Cordilleran trend with the exception of Al_2O_3. Therefore, even if melts do not plot in the Cordilleran trend, magmas comprising these melts are likely to fall within the trend if they contain an adequate

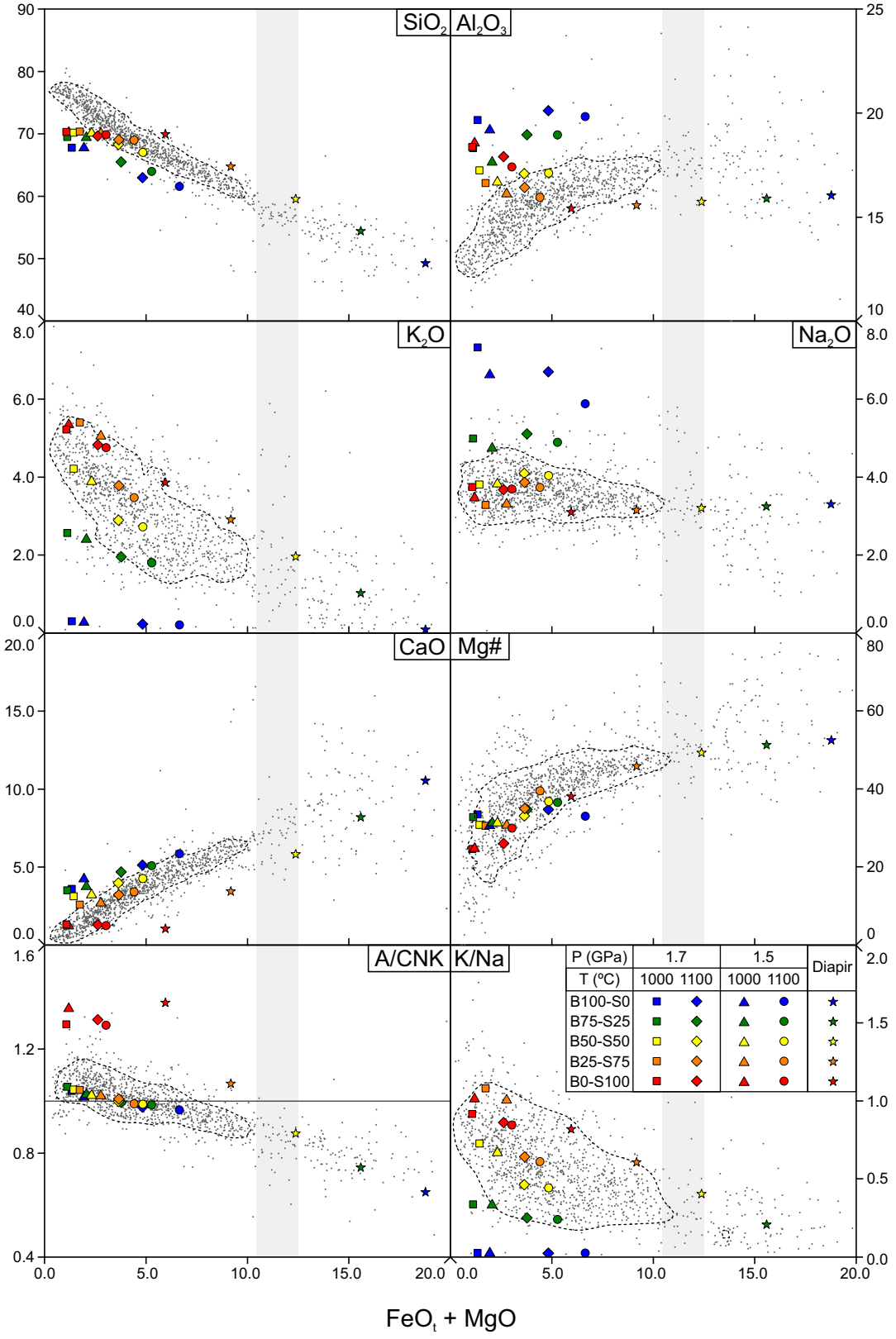

Fig. 9. Composition of the melts modelled at 1000 °C and 1.7 GPa (squares), 1100 °C and 1.7 GPa (diamonds), 1000 °C and 1.5 GPa (triangles) and 1100 °C and 1.5 GPa (circles), plotted against the Cordilleran trend. The dashed line contours 80% of the granitoids in a kernel density distribution. Note that only the modelled melt compositions produced at 1100 °C at 1.5 and 1.7 GPa from diapirs with a basalt:sediment proportion of 50:50 and 25:75 plot always within the contour line for all elements and element ratios.

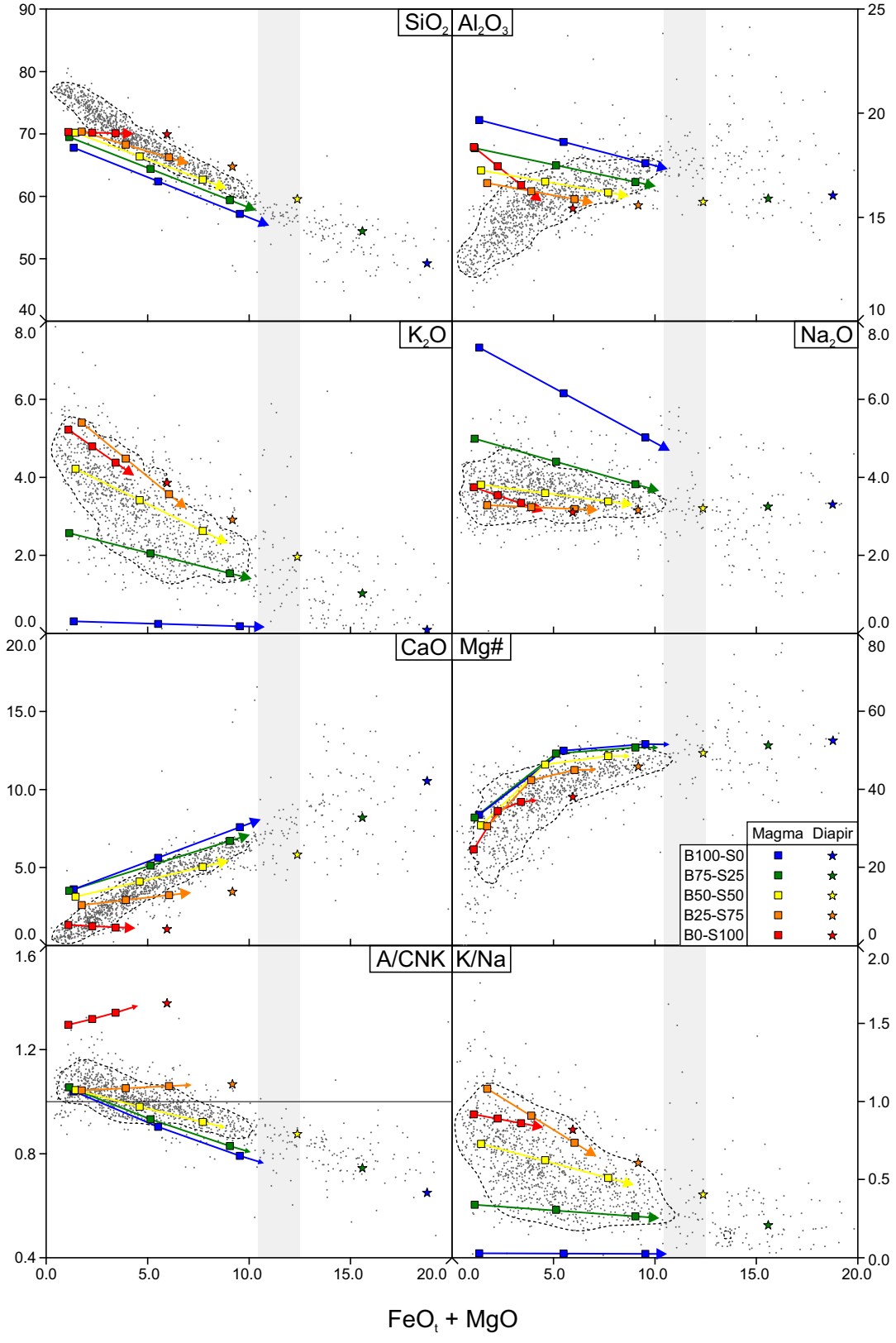

Fig. 10. Composition of the modelled magmas formed by restite unmixing with 0, 20 and 40 wt% entrained minerals modelled at 1000 °C and 1.7 GPa, plotted against the Cordilleran trend. The arrow points to a higher restite content in the magmas. The dashed line contours 80% of the granitoids in a kernel density distribution. Note that many modelled magma compositions, particularly from diapirs with a basalt:sediment proportion of 50:50 and 25:75, plot always within the contour line for all elements and element ratios.

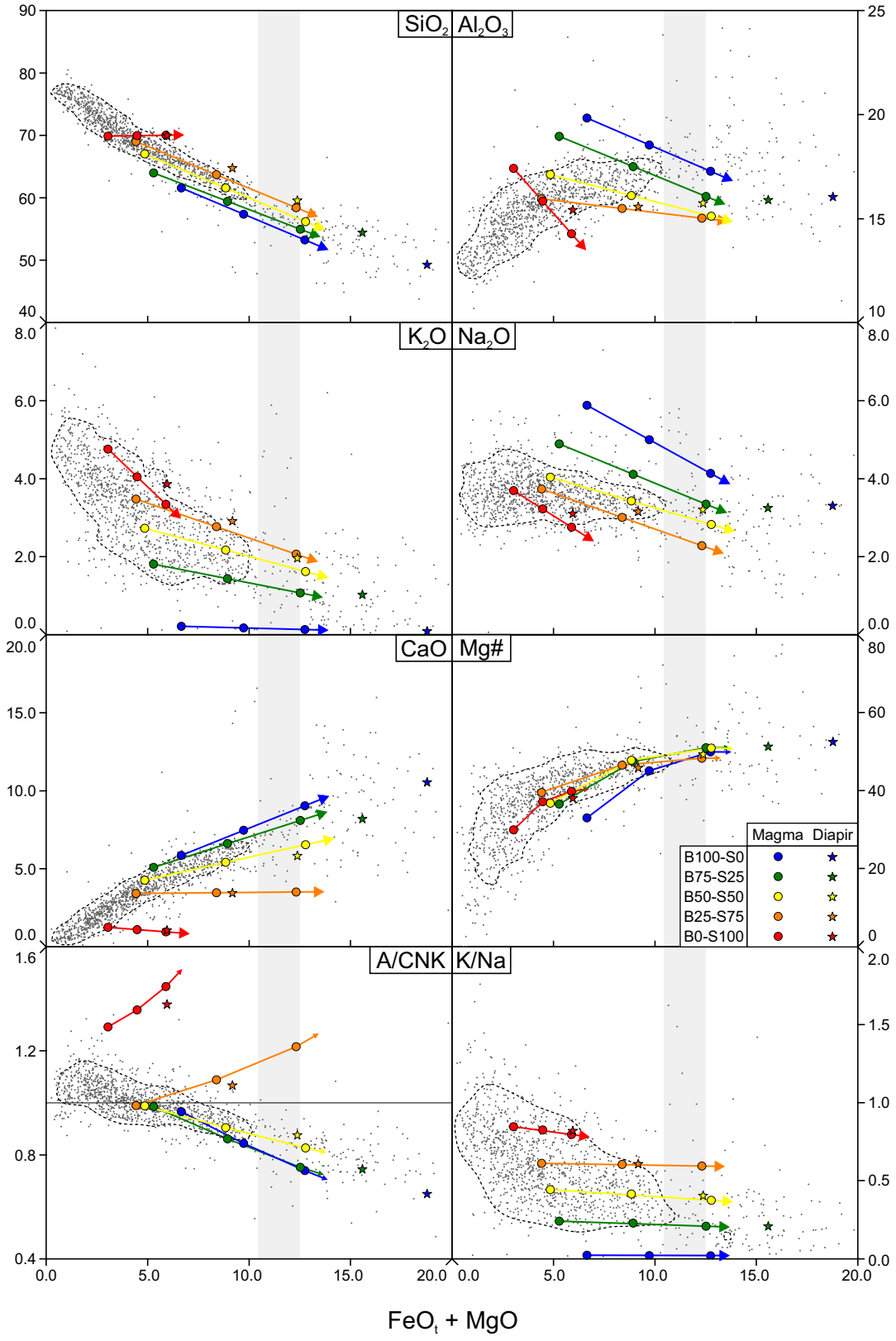

Fig. 11. Composition of the modelled magmas formed by restite unmixing with 0, 20 and 40 wt% entrained minerals modelled at 1100 °C and 1.5 GPa, plotted against the Cordilleran trend. The arrow points to a higher restite content in the magmas. The dashed line contours 80% of the granitoids in a kernel density distribution. Note that only the composition of modelled melts and restite-poor magmas, particularly from diapirs with a basalt:sediment proportion of 50:50 and 25:75, plot within the contour line for all elements and element ratios, compared to the case at 1000 °C and 1.5 GPa (Fig. 10).

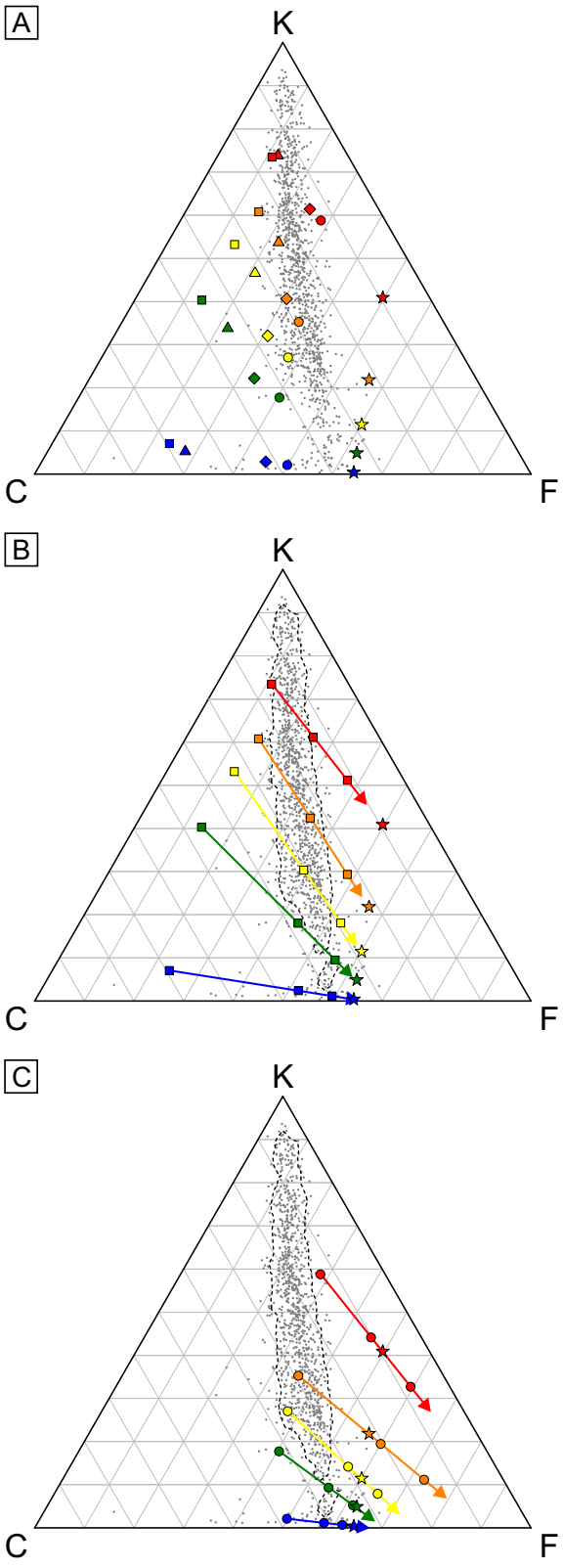

P (GPa)	1.7		1.5		Diapir
T (°C)	1000	1100	1000	1100	
B100-S0	■	◆	▲	●	★
B75-S25	■	◆	▲	●	★
B50-S50	□	◇	△	○	☆
B25-S75	■	◆	▲	●	★
B0-S100	■	◆	▲	●	★

(caption on next column)

Fig. 12. Composition of all modelled melts (A) and restite-bearing magmas with 0, 20 and 40 wt% entrained minerals modelled at 1000 °C and 1.7 GPa (B) and 1100 °C and 1.5 GPa (C), plotted against the Cordilleran trend in a K-C-F pseudoternary diagram. K is $2{\cdot}K_2O$, C is CaO – 10/3 P_2O_5 and F is $2{\cdot}Fe_2O_3$ + FeO + MgO, all in moles. The arrow points to a higher restite content in the magmas. The composition of the sources (stars) is also included. The dashed line contours 80% of the granitoids in a kernel density distribution. Note that for lower temperature systems, a larger proportion of restite is required to be entrained in the magmas in order for the compositions of the magmas to plot within the contour line.

amount of restites, expanding the P-T range of the parental magmas of Cordilleran granitoids and associated rocks to lower temperatures. The fact that restite-bearing magmas formed at 1000 °C must contain more restites (20–40 wt%) than the magmas formed at 1100 °C (0–20 wt%) to plot in the Cordilleran trend (Figs. 10 to 12) may just reflect the fact that the amount of restites in lower-T relaminated diapirs is higher than in higher-T diapirs. This inference will be studied in more detail in the next section.

Finally, magmas with ~30 wt% entrained minerals formed at 1100 °C and 1.5 and 1.7 GPa have a maficity that matches the compositional gap. They also have H_2O contents in the 1.5–2.3 wt% range, near the estimated maximum 2 wt% H_2O content of Castro (2013) and the H_2O content of andesitic melts in magma chambers (e.g. Kovalenko et al., 2000; Okumura, 2011), due to the lowering of the H_2O content of the magma caused by the entrainment of a nearly or completely anhydrous mineral assemblage. However, this 30% restite content of magmas at these P-T conditions is virtually identical to the restite content of diapirs with 50% sedimentary content or higher at the same P-T conditions (Table 4 in Appendix B), essentially meaning that the gap has the composition of relaminated diapirs, as proposed by Castro (2013) and Castro et al. (2013), and not of melts segregated from the diapirs, and that the relaminated diapirs contain ~50% sediment component. These conclusions are in agreement with our previous finding that only diapirs with a significant sediment component are able to form and detach from the subducting slab (section 5.1). They are also in agreement with mass balance calculations made by Castro et al. (2021) on the isotopic compositions of the North Patagonian batholith, with sediment contents in the range of 20–70% for several plutons, and with their finding of a match between the lack of sediment/crust erosion and subduction (diapirs would be rich in basaltic component) and a drastic reduction in magma productivity in the same batholith during the Late Cretaceous.

5.3. Restite entrainment and the compositional variability of continental arc magmatism

The similarities between the compositional trends of the modelled magmas with increasing amounts of entrained minerals and the Cordilleran trend raises the question whether the composition of the magmas produced by mineral entrainment represents only the composition of the parental magmas prior to a posterior evolution, or the final composition of the magmatic rocks without the need for other composition-modifying processes like fractional crystallization. Our results suggest that restite entrainment alone cannot produce the whole compositional distribution of Cordilleran rocks, for the following reasons: (1) the lack of any parallelism in the trends for the Al_2O_3 content between the modelled magmas and the granitoids (Figs. 10 and 11): if restite entrainment is the main process, trends would be parallel for all elements (García-Arias, 2018; García-Arias and Stevens, 2017); (2) no modelled melt or magma has a SiO_2 content above 70.5 wt% on an anhydrous basis (Figs. 8 to 11), whilst ~35% of the granitoids have a higher SiO_2 content (Fig. 3): restite entrainment reduces, not increases, the SiO_2 content of the magmas; and (3) using another projection for the composition of the modelled melts and magmas, like the K_2O-CaO-(FeO_t + MgO) pseudoternary diagram, clearly shows that the modelled compositional trends are not parallel to the Cordilleran trend (Fig. 12).

Our conclusion is that restite entrainment alone is not the main process in the compositional distribution of the Cordilleran granitoids and associated rocks but it is necessary to produce rocks more mafic than granodiorites, as explained below.

At this point, the conclusions of the work of García-Arias and Stevens (2017a) on filter-pressing fractional crystallization (the model advocated by Castro, 2013 for fractional crystallization in Cordilleran plutons) are useful in understanding the combination of restite entrainment and fractional crystallization. These authors found that the compositional trends of parental magmas and of fractionated bodies are very similar, and that the maximum maficity of fractionated magmas produced by filter-pressing is only twice the maficity of the parental melt or magma. Therefore, fractionation of felsic (granodioritic) melts cannot produce mafic (gabbroic) rocks, but fractionation of restite-bearing intermediate magmas can produce such mafic bodies; moreover, fractionation of restite-bearing intermediate magmas can produce fractionated felsic melts whose composition is very similar to unfractionated felsic parents, be they melts or magmas (Garcia-Arias and Stevens, 2017, their Fig. 12). Moreover, if the composition of the parental melts or magmas do not fall within the granitoid trend, the trends produced by fractional crystallization will not match those of the granitoids and associated rocks (Garcia-Arias and Stevens, 2017, their Fig. 13). In other words, what creates the compositional trend that S- and I-type granites show with increasing maficity is the composition of several parental melts or magmas, not fractional crystallization (of the filter-pressing type).

Under this conclusion, the Cordilleran trend is controlled by the composition of the melts and magmas that segregate from the relaminated diapirs: fractional crystallization only increases the compositional range. Melts formed from the diapirs with 50:50 and 25:75 basalt: sediment ratio at 1100 °C plot in the trend (Figs. 11 and 12C), whilst melts formed from the same diapirs but at 1000 °C only plot in the Cordilleran trend if they contain between 20 and 40 wt% entrained restites (Figs. 10 and 12B). At 1100 °C the amount of melt in those diapirs ranges from ~69 to ~84 wt% (~76 to ~89 vol%, respectively) and thus the amount of restites is ~31–16 wt% (~24–11 vol%), whilst at 1000 °C the amount of melt ranges from ~43 to ~50 wt% (~51 to ~56 vol%) and the amount of restites is ~57–50 wt% (~49–44 vol%) (Table 3 in Appendix B). Given that restites are in suspension within the melt in the relaminated diapirs, it seems plausible that the higher the amount of restite in the diapir the higher the amount of restite able to be segregated with the melt. Therefore, there exists a temperature-restite proportion relationship that controls the composition of the parental magmas. In other words, temperature is the main factor that ultimately controls the Cordilleran trend because temperature controls the amount of restites, which in turn controls the restite content of the parental magmas that segregate from the diapirs, prior to fractional crystallization.

Regarding the compositional gap in the maficity and silica distributions (Fig. 3), the temperature-amount of restite relationship and the conclusions of García-Arias and Stevens (2017a) indicate that the compositional trend created by fractionation or cotectic evolution of that parental magma coincides with the composition of more felsic parental restite-bearing magmas. Consequently, the existence of these less mafic parental magmas was obscured. This conclusion also explains why compositions more felsic than the gap are more abundant than expected from the amount of the most mafic compositions if the felsic compositions derived solely by cotectic evolution of the compositions from the gap (see section 2): these most mafic compositions can only be produced by fractionation of the most mafic parental magmas, whilst the more felsic composition in the Cordilleran trend comprise felsic parental magmas plus felsic fractionated bodies. Moreover, if equilibrium or fractional crystallization produces a scatter in the fractionated mafic bodies as described by Castro (2013), the scatter in the fractionated bodies of parental felsic magmas will be obscured by the linear trend of the parental restite-bearing magmas. Conversely, the fractionated mafic bodies of the most mafic parental magmas have compositions that do not match any of the parental melts/magmas and thus the scatter becomes apparent. Under these conclusions, the 10.5–12.5 wt% maficity gap that separates a linear felsic trend and a scattered mafic cloud is not the composition of the only parental magma of all granitoids (as interpreted by Castro, 2013 and Castro et al., 2013) but the uppermost maficity limit of the parental magmas which, as stated above, is the maficity of the relaminated diapirs from which these parental magmas separate and ascend through the crust. In other words, the maficity of the parental magmas prior to fractional crystallization or cotectic evolution ranges from ~1 wt% (the maficity of the most felsic modelled melts, Fig. 8, Table 3 in Appendix B) to ~11.5 wt%.

In summary, our modelling shows that the bulk of the melts produced have a composition consistent with the bulk granodioritic composition of the Cordilleran magmatism, and that the compositional gap represents the composition of the diapirs from which the parental magmas of the Cordilleran rocks segregate. Therefore, the models of Castro et al. (2010) and Castro (2013) and Castro et al. (2013) are not contradictory but complementary. Given the restricted compositional range of the gap, the diapirs that relaminate to the base of the crust must also have a restricted composition, and this composition coincides with diapirs containing 50–60% sediment component (Fig. 8), a conclusion that agrees with the estimated sediment contents of the North Patagonian batholith, of 20–70 wt% (Castro et al., 2021). Finally, we propose that the proportion of sediment in the mélange and the degree of hydration of the mantle play a major role in the ability of diapirs to detach from the slab, as this sediment proportion and mantle hydration influence the density of the mélange and the mantle, respectively, and their relative difference. If the maximum amount of basaltic component in the mélange is 50% for diapirs to ascend, then the mantle at 3.0–3.5 GPa must not have H_2O contents higher than 2 wt% because dry mélanges with 50% basaltic component or higher are denser than the mantle with this 2 wt% H_2O content (Fig. 7A); if mélanges are wet, the mantle wedge may be slightly more hydrated (Fig. 7B). Mélanges containing a sediment component higher than 60% may be too less dense to be subducted to depths equivalent to 3.0–3.5 GPa and would ascend up along the subduction channel (e.g. Gerya et al., 2008).

6. Conclusions

The mélange diapir model is a plausible process to explain the generation of magmatism in continental arcs and their compositional variability. For translithospheric diapirs to form, they must contain ~50% of sedimentary component, based on buoyancy and compositional constraints. The results of our modelling indicate that the main control on the composition of the parental magmas prior to fractional crystallization or cotectic evolution (and thus the compositional variability of the Cordilleran granitoids and associated rocks) is the amount of restites entrained, which in turn depends on the temperature of the region of the relaminated diapir from which the magma pulse segregates: the lower the temperature of the segregated pulse, the higher the amount of restites entrained. Despite this first-order control of the temperature-amount of restite relationship in the composition of the parental magmas, fractional crystallization or cotectic evolution are still needed to account for the whole compositional range observed in Cordilleran rocks.

Declaration of Competing Interest

The authors declare that they have no known competing financial interests or personal relationships that could have appeared to influence the work reported in this paper.

Acknowledgements

The authors want to thank Prof. J.-F. Moyen, Prof. C.F. Miller and an

anonymous reviewer for their work. This investigation was funded by internal funds of the University of Los Andes, Colombia (FAPA – Fondo de Ayuda a Profesores Asistentes), FAPA number INV- 2019-63-1701.

Appendix A. Supplementary data

Supplementary data to this article can be found online at https://doi.org/10.1016/j.lithos.2022.106881.

References

Behn, M.D., Kelemen, P.B., Hirth, G., Hacker, B.R., Massonne, H.-J., 2011. Diapirs as the source of the sediment signature in arc lavas. Nat. Geosci. 4, 641–646.

Blanco-Quintero, I.F., Gerya, T., García-Casco, A., Castro, A., 2011. Subduction of young oceanic plates: a numerical study with application to aborted thermal-chemical plumes. Geochem. Geophys. Geosyst. 12, Q10012. https://doi.org/10.1029/2011GC003717.

Brounce, M.N., Kelley, K.A., Cottrell, E., 2014. Variations in $Fe^{3+}/\Sigma Fe$ of Mariana arc basalts and mantle wedge fO_2. J. Petrol. 55, 2513–2536.

Castro, A., 2013. Tonalite–granodiorite suites as cotectic systems: a review of experimental studies with applications to granitoid petrogenesis. Earth Sci. Rev. 124, 68–95.

Castro, A., 2014. The off-crust origin of granite batholiths. Geosci. Front. 5, 63–75.

Castro, A., 2020. The dual origin of I-type granites: The contribution from experiments. In: Janoušek, V., Bonin, B., Collins, W.J., Farina, F., Bowden, P. (Eds.), Post-Archean Granitic Rocks: Petrogenetic Processes and Tectonic Environments, Geological Society of London, Special Publication, 491, pp. 101–145.

Castro, A., Gerya, T.V., 2008. Magmatic implications of mantle wedge plumes: experimental study. Lithos 103, 138–148.

Castro, A., Corretge, L.G., El-Biad, M., El-Hmidi, H., Fernandez, C., Patiño Douce, A.E., 2000. Experimental constraints on Hercynian anatexis in the Iberian Massif, Spain. J. Petrol. 41, 1471–1488.

Castro, A., Gerya, T.V., García-Casco, A., Fernández, C., Diaz-Alvarado, J., Moreno-Ventas, I., Löw, I., 2010. Melting relations of MORB-sediment mélanges in underplated mantle wedge plumes. Implications for the origin of cordilleran-type batholiths. J. Petrol. 51, 1267–1295.

Castro, A., Vogt, K., Gerya, T.V., 2013. Generation of new continental crust by sublithospheric silicic-magma relamination in arcs: a test of Taylor's andesite model. Gondwana Res. 23, 1554–1556.

Castro, A., Rodríguez, C., Fernández, C., Aragón, E., Pereira, M.F., Molina, J.F., 2021. Secular variations of magma source compositions in the North Patagonian batholith from the Jurassic to Tertiary: was mélange melting involved? Geosphere 17, 766–785.

Cawood, P.A., Hawkesworth, C.J., Dhuime, B., 2013. The continental record and the generation of continental crust. GSA Bull. 125, 14–32.

Codillo, E.A., Le Roux, V., Marschall, H.R., 2018. Arc-like magmas generated by mélange-peridotite interaction in the mantle wedge. Nat. Commun. 9, 2864.

Connolly, J.A.D., 2009. The geodynamic equation of state: what and how. Geochem. Geophys. Geosyst. 10, Q10014.

Cottrell, E., Kelley, K.A., 2011. The oxidation state of Fe in MORB glasses and the oxygen fugacity of the upper mantle. Earth Planet. Sci. Lett. 305, 270–282.

Fuhrman, M.L., Lindsley, D.H., 1988. Ternary-feldspar modeling and thermometry. Am. Mineral. 73, 201–215.

García-Arias, M., 2018. Decoupled Ca and Fe + Mg content of S-type granites: an investigation on the factors that control the Ca budget of S-type granites. Lithos 318–319, 30–46.

García-Arias, M., 2020. Consistency of the activity–composition models of Holland, Green, and Powell (2018) with experiments on natural and synthetic compositions: a comparative study. J. Metamorph. Geol. 38, 993–1010.

Garcia-Arias, M., Stevens, G., 2017. Phase equilibrium modelling of granite magma petrogenesis: B. An evaluation of themagma compositions that result from fractional crystallization. Lithos 277, 109–130.

García-Arias, M., Stevens, G., 2017. Phase equilibrium modelling of granite magma petrogenesis: A. An evaluation of the magma compositions produced by crystal entrainment in the source. Lithos 277, 131–153.

Gerya, T.V., Stöckhert, B., 2006. Two-dimensional numerical modeling of tectonic and metamorphic histories at active continental margins. Int. J. Earth Sci. 95, 250–274.

Gerya, T.V., Yuen, D.A., 2003. Rayleigh-Taylor instabilities from hydration and melting propel cold plumes at subduction zones. Earth Planet. Sci. Lett. 212, 47–62.

Gerya, T.V., Perchuk, L.L., Burg, J.-P., 2008. Transient hot channels: Perpetrating and regurgitating ultrahigh-pressure, high-temperature crust–mantle associations in collision belts. Lithos 103, 236–256.

Green, E.C.R., Holland, T.J.B., Powell, R., 2007. An order-disorder model for omphacitic pyroxenes in the system jadeite-diopside-hedenbergite-acmite, with applications to eclogite rocks. Am. Mineral. 92, 1181–1189.

Green, E.C.R., White, R.W., Diener, J.F.A., Powell, R., Holland, T.J.B., Palin, R.M., 2016. Activity-composition relations for the calculation of partial melting equilibria in metabasic rocks. J. Metamorph. Geol. 34, 845–869.

Hacker, B.R., Kelemen, P.B., Behn, M.D., 2011. Differentiation of the continental crust by relamination. Earth Planet. Sci. Lett. 307, 501–516.

Hervé, F., Pankhurst, R.J., Fanning, C.M., Calderon, M., Yaxley, G.M., 2007. The south Patagonian batholith: 150 my of granite magmatism on a plate margin. Lithos 97, 373–394.

Holland, T.J.B., Powell, R., 2003. Activity-composition relations for phases in petrological calculations: and asymmetric multicomponent formulation. Contrib. Mineral. Petrol. 145, 492–501.

Holland, T.J.B., Powell, R., 2011. An improved and extended internally consistent thermodynamic dataset for phases of petrological interest, involving new equations of state for solids. J. Metamorph. Geol. 29, 333–383.

Holland, T.J.B., Green, E.C.R., Powell, R., 2018. Melting of peridotites through to granites: a simple thermodynamic model in the system KNCFMASHTOCr. J. Petrol. 59, 881–900.

Jagoutz, O., Kelement, P.B., 2015. Role of arc processes in the formation of continental crust. Annu. Rev. Earth Planet. Sci. 43, 363–404.

Kemp, A.I.S., Hawkesworth, C.J., 2003. Granitic perspectives on the generation and secular evolution of the continental crust. In: Holland, H.D., Turekian, K.K. (Eds.), Treatise on Geochemistry. Elsevier-Pergamon Oxford, v. 3.11, pp. 349–410.

Kovalenko, V.I., Naumov, V.B., Yarmolyuk, V.V., Dorofeeva, V.A., 2000. Volatile components (H_2O, CO_2, Cl, F, and S) in magmas of intermediate and acid compositions from distinct geodynamic settings: evidence from melt inclusions and chill glasses. Petrology 8, 525–556.

Kress, V.C., Carmichael, I.S.E., 1991. The compressibility of silicate liquids containing Fe_2O_3 and the effect of composition, temperature, oxygen fugacity and pressure on their redox states. Contrib. Mineral. Petrol. 108, 82–92.

Le Maitre, R.W., 1976. The chemical variability of some common igneous rocks. J. Petrol. 17, 589–598.

Lee, C.-T.A., Morton, D.M., Kistler, R.W., Baird, A.K., 2007. Petrology and tectonics of Phanerozoic continent formation: from island arcs to accretion and continental arc magmatism. Earth Planet. Sci. Lett. 263, 370–387.

Lee, C.-T.A., Luffi, P., Le Roux, V., Dasgupta, R., Albaréde, F., Leeman, W.P., 2010. The redox state of arc mantle using Zn/Fe systematics. Nature 468, 681–685.

Lin, C.-H., Shih, M.-H., Lai, Y.-C., 2021. Mantle wedge diapirs detected by a dense seismic array in Northern Taiwan. Sci. Rep. 11, 1561.

López, S., Castro, A., 2001. Determination of the fluid-absent solidus curve and supersolidus phase relationships of MORB-derived amphibolites in the range 4-14 kbar. Am. Mineral. 86, 396–403.

Malaspina, N., Poli, S., Fumagalli, P., 2009. The oxidation state of metasomatized mantle wedge: insights from C–O–H-bearing garnet peridotite. J. Petrol. 50, 1533–1552.

Martínez Ardila, A.M., Clausena, B.J., Memeti, V., Paterson, S.R., 2019. Source contamination, crustal assimilation, and magmatic recycling duringthree flare-up events in the cretaceous Peruvian Coastal Batholith: an example from the Ica-Pisco plutons. J. S. Am. Earth Sci. 95, 102300.

Massonne, H.-J., Willner, A.P., 2008. Phase relations and dehydration behaviour of psammopelite and mid-ocean ridge basalt at very-low-grade to low-grade metamorphic conditions. Eur. J. Mineral. 20, 867–879.

Okumura, S., 2011. The H_2O content of andesitic magmas from three volcanoes in Japan, inferred from the infrared analysis of clinopyroxene. Eur. J. Mineral. 23, 771–778.

Padrón-Navarta, J.A., López Sánchez-Vizcaíno, V., Hermann, J., Connolly, J.A.D., Garrido, C.J., Gómez-Pugnaire, M.T., Marchesi, C., 2013. Tschermak's substitution in antigorite and consequences for phase relations and water liberation in high-grade serpentinites. Lithos 178, 186–196.

Pankhurst, R.J., Weaver, S.D., Herve, F., Larrondo, P., 1999. Mesozoic-cenozoic evolution of the North Patagonian batholith in Aysen, southern Chile. J. Geol. Soc. 156, 673–694.

Parkinson, I.J., Arculus, R.J., 1999. The redox state of subduction zones: insights from arc-peridotites. Chem. Geol. 160, 409–423.

Patiño Douce, A.E., 1999. What do experiments tell us about the relative contributions of crust and mantle to the origin of granitic magmas? In: Castro, A., Fernandez, C., Vigneresse, J.L. (Eds.), 1999. Understanding Granites - Integrating New and Classical Techniques, pp. 55–76. Geological Society of London Special Publications 168.

Patiño Douce, A.E., 2005. Vapor-absent melting of tonalite at 15–32 kbar. J. Petrol. 46, 275–290.

Patiño Douce, A.E., Beard, J.S., 1995. Dehydration-melting of biotite gneiss and quartz amphibolite from 3 to 15 kbar. J. Petrol. 36, 707–738.

Richards, J.P., 2015. The oxidation state, and sulfur and Cu contents of arc magmas: implications for metallogeny. Lithos 233, 27–45.

Rosenberg, C.L., Handy, M.R., 2005. Experimental deformation of partially melted granite revisited: implications for the continental crust. J. Metamorph. Geol. 23, 19–28.

Rossetti, F., Nasrabady, M., Vignaroli, G., Theye, T., Gerdes, A., Razavi, M.H., Vaziri, H. M., 2010. Early cretaceous migmatitic mafic granulites from the Sabzevar range (NE Iran): implications for the closure of the Mesozoic peri-Tethyan oceans in central Iran. Terra Nova 22, 26–34.

Rudnick, R.L., Gao, S., 2003. Composition of the continental crust. In: Holland, H.D., Turekian, K.K. (Eds.), Treatise on Geochemistry, v. 3.1. Elsevier-Pergamon, Oxford, pp. 1–64.

Sorensen, S.S., Barton, M.D., 1987. Metasomatism and partial melting in a subduction complex: Catalina Schist, southern California. Geology 15, 115–118.

Stevens, G., Villaros, A., Moyen, J.-F., 2007. Selective peritectic garnet entrainment as the origin of chemical diversity in S-type granites. Geology 35, 9–12.

Takahashi, E., 1986. Melting of a dry peridotite KLB-1 up to 14 GPa: implications on the origin of peridotitic upper mantle. J. Geophys. Res. 91, 9367–9382.

Taylor, S.R., 1967. The origin and growth of continents. Tectonophysics 4, 17–34.

Taylor, S.R., McLennan, S.M., 1985. The Continental Crust: Its Composition and Evolution. Blackwell Scientific Publications, Oxford, 312 pp.

Vogt, K., Gerya, T.V., Castro, A., 2012. Crustal growth at active continental margins: numerical modeling. Phys. Earth Planet. Inter. 192–193, 1–20.

Vogt, K., Castro, A., Gerya, T.V., 2013. Numerical modelling of geochemical variations caused by crustal relamination. Geochem. Geophys. Geosyst. 14, 470–487.

Welch, M.D., 2020. Amphiboles. In: Encyclopedia of Geology, , second ed.v. 1, pp. 297–300. https://doi.org/10.1016/b978-0-08-102908-4.00095-3.
White, A.J.R., Chappell, B.W., 1977. Ultrametamorphism and granitoid genesis. Tectonophysics 43, 7–22.
White, R.W., Powell, R., Holland, T.J.B., Worley, B.A., 2000. The effect of TiO_2 and Fe_2O_3 on metapelitic assemblages at greenschist and amphibolite facies conditions: Mineral equilibria calculations in the system K_2O-FeO-MgO-Al_2O_3-SiO_2-H_2O-TiO_2-Fe_2O_3. J. Metamorph. Geol. 18, 497–512.
White, R.W., Powell, R., Holland, T.J.B., Johnson, T.E., Green, E.C.R., 2014. New mineral activity-composition relations for thermodynamic calculations in metapelitic systems. J. Metamorph. Geol. 32, 261–286.
Whitney, D.L., Evans, B.W., 2010. Abbreviations for names of rock-forming minerals. Am. Mineral. 95, 185–187.
Winter, J.D., 2001. An Introduction to Igneous and Metamorphic Petrology. Prentice Hall, New Jersey, p. 697.